

**Griffith School of Engineering
Griffith University**

6002ENG – Industry Affiliates Program

Investigation into Near Zero Power Bushfire Early Detection

Ethan Smith, s5164398

Date, Trimester 2, 2022

Academic Supervisor: Yong Zhu

A report submitted in partial fulfilment of A Bachelor of Engineering (Honours)

The copyright on this report is held by Ethan Smith. Permission has been granted to Griffith University to keep a reference copy of this report.



EXECUTIVE SUMMARY

The main current early bushfire detection methods are the use of satellites and wireless sensor networks. While satellite detection offers consistently accurate bushfire detection during clear weather, during low visibility mainly due to clouds, it is unable to provide accurate detection of bushfires. Wireless sensor networks, offer consistently accurate detection of bushfires through all weather conditions. However, these networks consume power and therefore require frequent maintenance to replace batteries etc. Over an entire network, this becomes a tedious and laboursome task. Therefore, this thesis focuses on designing and testing a near zero-power wireless sensor node which would offer the upside of wireless sensor networks, without the required maintenance.

The first stage of the project was to review the existing literature on bushfire detection to determine the best solutions for long range communication and zero-power usage. It was found that LoRaWAN offers low-power, long-range communication and a thermal mechanical switch can be used to consume no power prior to detecting a fire.

After this device was constructed, the next stage was to prove the concept of the design by testing both the LoRaWAN node and the thermal switch. The results of this thesis showed that LoRaWAN was capable of transmitting long-range signals in various environments and therefore offered a viable solution for the node. They also showed that the thermal mechanical switch was consistently able to detect a fire, while offering zero-power consumption prior to detection.

The final objective was to evaluate the results, focussing on what future work can be done to improve the solution. This found that the only significant drawback to the design was the inability for the node to be used in a mesh system. Therefore, future work to remedy this problem would offer a early bushfire detection solution without any significant drawbacks.

ACKNOWLEDGEMENTS

I would like to acknowledge the various types of support I have received throughout testing and writing this thesis.

- Dr Yong Zhu, thank you for your ongoing support and guidance throughout this thesis. Weekly meetings to discuss progress and set goals allowed me to stay on track throughout the trimester. Your technical support was very helpful, as I pursued a thesis with some major electrical elements, I could not have done this without you.
- My friends and family, thank you for your selfless support, assisting with the tedious, ongoing experiments. You gave up your time to help me collect the results for this thesis and I could not have done it without you.
- Dr Ivan Gratchev, thank you for your support with helpful lectures how to write the thesis. You offered great help with an unfamiliar assessment item.

To everyone else not mentioned above, thank you for your support. I could not have done this thesis alone.

TABLE OF CONTENTS

EXECUTIVE SUMMARY.....	I
TABLE OF CONTENTS.....	III
LIST OF FIGURES	IV
LIST OF TABLES	V
1 INTRODUCTION.....	6
1.1 General.....	6
1.2 Background Information.....	6
1.3 Aims and Objectives	7
2 REVIEW OF PUBLISHED LITERATURE.....	8
2.1 Introduction.....	8
2.2 Bushfire Detection Solutions.....	8
2.2.1 Satellite-based Detection.....	9
2.2.2 Wireless Sensor Networks	12
2.3 LoRaWAN	15
2.4 Zero-Power Switch.....	17
2.5 Summary.....	19
3 METHODOLOGY.....	20
3.1 Design Process	20
3.2 LoRaWAN Experimental.....	23
3.3 Thermal Mechanical Switch Experiment	27
4 EXPERIMENTAL RESULTS.....	32
4.1 LoRaWAN Distance Testing.....	32
4.1.1 Free Space (Line of Sight) Test.....	33
4.1.2 Urban Test.....	35
4.1.3 Bush Test.....	37
4.2 LoRaWAN Discussion	39
4.2.1 Free Space Test	39
4.2.2 Urban Test.....	40
4.2.3 Bush Test.....	41
4.2.4 Summary	42
4.3 Thermal Switch Testing	44

4.4 Thermal Switch Discussion	44
5 CONCLUSIONS	46
6 REFERENCES.....	48
7 APPENDICES	52
 7.1 Appendix 1 – Arduino IDE Code	52
7.1.1 LoRaWAN Shield Code.....	52
7.1.2 LoRaWAN Gateway Code.....	54
 7.2 LoRaWAN Distance Testing Results	57
7.2.1 Free Space Test Results.....	57
7.2.2 Urban Test Results	58
7.2.3 Bush Test Results	59

LIST OF FIGURES

Figure 1 - Relationship between emitted spectral radiance and emitted temperature for the MIR and TIR spectral bands (Jones et al., 2017)	10
Figure 2 - WSN for real time forest fire detection (Yu et al., 2005).....	12
Figure 3 - Wireless Sensor Node Schematic for Experiment by Antunes et al. (2019).....	13
Figure 4 - LoRaWAN System Flowchart (Casals et al., 2017).....	15
Figure 5 - Summary of Communication Technologies (Mayer et al., 2019)	16
Figure 6 - MEMS Switch in OFF State (Jaafar et al., 2014).....	17
Figure 7 - MEMS Switch in ON State (Jaafar et al., 2014)	17
Figure 8 - Thermal Actuated MEMS Switch (Li et al., 2010)	18
Figure 9 - Zero Power WSN Design	20
Figure 10 - LoRaWAN Node with Thermal Mechanical Switch.....	21
Figure 11 - LoRaWAN Node Signal Demodulated by Gateway and Displayed on Laptop....	22
Figure 12 - Gateway Powered from Car Battery.....	23
Figure 13 - Free Space Test Schematic	24
Figure 14 - Urban Test Schematic.....	25
Figure 15 - Bush Test Schematic	26
Figure 16 - Working Principle of Thermal Mechanical Switch.....	27
Figure 17 - LoRaWAN Node Circuit with Multimeter in Parallel	29
Figure 18 - LoRaWAN Node Circuit with Multimeter in Series	29

Figure 19 - Thermal Mechanical Switch Experimental Setup	30
Figure 20 - Gateway Listening for Signal from Node	31
Figure 21 - Signal Power over Distance (Eric, 2018)	32
Figure 22 - RSSI over Distance for Free Space Test	33
Figure 23 - SNR over Distance for Free Space Test	34
Figure 24 - RSSI over Distance for Urban Test	35
Figure 25 - SNR over Distance for Urban Test.....	36
Figure 26 - RSSI over Distance for Bush Test.....	37
Figure 27 - SNR over Distance for Bush Test	38
Figure 28 - Free Space Test Data Point Map (Google Maps, 2022).....	39
Figure 29 - Urban Test Data Point Map (Google Maps, 2022).....	40
Figure 30 - Bush Test Data Point Map (Google Maps, 2022)	41

LIST OF TABLES

Table 1 - Summary of LoRaWAN Performance across Environments	42
Table 2 - Results of Thermal Switch Testing.....	44
Table 3 - LoRaWAN Free Space Test Raw Data.....	57
Table 4 - LoRaWAN Urban Test Raw Data	58
Table 5 - LoRaWAN Bush Test Raw Data	59

1 INTRODUCTION

1.1 General

Bushfires have always occurred; however, the effects of climate change have seen a significant increase in the frequency of these fires. They are continuing to pose growing threats to human safety as well as natural resources and habitats around the world (Finney, 2021). The effect of increasing bushfires is significant and widespread. Due to the continued loss of lives, structures and nature, new and improved detection of these fires offers a wide range of benefits. For these reasons, interest from a range of engineering disciplines with many possible solutions has increased over the last few years.

1.2 Background Information

The most widely accepted current solution to wildfire detection is the use of fire sensors in terrestrial satellites. Fire detection algorithms are used to detect and predict wildfire behaviour based on this satellite imaging. These algorithms produce numerous false alarms due to imperfect rejection of sun glint, forest clearing, and issues with some tentative pixels (Giglio et al., 2016). The most significant drawback of satellite fire detection is cloud cover causing both false alarms and undetected bushfires. As the algorithms attempt to detect fires, they reject cloud cover and therefore, bushfires occurring beneath clouds remain undetected.

To counter these drawbacks, Wireless Sensor Networks (WSNs) have been tested for fire detection. Individual wireless sensor nodes are equipped with various sensors to measure temperature, humidity, light intensity, and carbon monoxide (Dampage et al., 2022). These nodes can be placed over an entire forest to transmit information to the base station where the data can be analysed to detect bushfires and predict their behaviour. This solution offers a wider range of more accurate information compared to satellite detection. A drawback of WSNs is that they require batteries which need replacing when low. This is tedious and demanding considering the large number of nodes required to detect fires in an entire forest. Solar power is also flawed as no significant sunlight is available under many trees. Therefore, a solution which does not draw power would be beneficial.

The potential solution explored in this thesis is a WSN consisting of near-zero power nodes. Micro electromechanical systems (MEMS) technology has seen considerable growth over

recent years with numerous potential uses. One of these uses is a near-zero power system using a mechanical switch which only closes an electrical circuit when a signal of interest is present. This system therefore greatly reduces standby power consumption to near-zero which gives the device greatly extended battery life (Rajaram et al., 2018). The use of this technology would allow a network of nodes to be deployed over a large area without the need for frequent maintenance or monitoring of battery life.

1.3 Aims and Objectives

The overarching aim of this investigation is to develop a wireless sensor node capable of detecting a fire and transmitting a long-range signal to a base station with zero power usage prior to fire detection and to evaluate its performance.

The first objective is to review the existing literature on bushfire detection with a focus on long-range wireless communication and zero-power mechanical switches, to design a viable solution.

The second objective is to construct a wireless sensor node based on the design, consisting of a zero-power mechanical switch and long-range communication device.

The third objective is to prove the concept of the design by testing the range and reliability of the communication device and validating the thermal mechanical switch.

The fourth objective is to evaluate the performance of the device and to determine what improvements can be made in future work.

2 REVIEW OF PUBLISHED LITERATURE

2.1 Introduction

This section reviews relevant literature regarding current and emerging bushfire detection solutions, focusing on satellite-based detection and wireless sensor networks. Options for low power, long range wireless communication are then discussed, in terms of their performance for use in bushfire detection wireless sensor nodes. A research gap of wireless sensor nodes without the need for maintenance due to power usage is identified and discussed with a focus on zero-power thermal switches.

2.2 Bushfire Detection Solutions

The first method of bushfire detection was the use of fire towers. Remote lookouts were manned during peak fire seasons, providing directional based fire information. The main drawbacks of fire towers are the required manpower and the lack of detailed information they provide. Spotted planes offered more detailed fire information, however, the solution was expensive and limited by flying range (Jones et al., 2017). With the modern growth in technology, the range of methods for early bushfire detection is increasing. The most common of these methods is the use of satellite-imaging to detect and map fires. Satellite-imaging has been used for decades and continues to improve as new algorithms are developed. Wireless Sensor Networks (WSN) are another emerging method for early bushfire detection. These networks aim to deliver real time fire data, while not suffering from drawbacks which hinder satellite detection (Yu et al., 2005).

2.2.1 Satellite-based Detection

There are two products from the use of satellites in fire detection. The first is called “active fire detection”. In this process, satellite imaging is used in conjunction with various algorithms to flag pixels as either yes, where fire is detected, or no, where no fire is detected. The second characterises the pixel as flaming, smouldering or unburned. The temperature or fire radiative power is also assigned to the pixel (Csiszar et al., 2018).

Detection of bushfires mainly uses the middle infrared (MIR) ($3\text{-}5\mu\text{m}$) and the thermal infrared (TIR) ($8\text{-}14\mu\text{m}$) channels of remote sensing imagery. The principles of this bushfire detection are based on Planck law, Wien’s displacement law, and Stefan-Boltzmann law (Hua, Shao, 2017).

All objects emit an electromagnetic radiation which can be approximated as the black body radiation. The wavelength of this radiation is dependent on the temperature of the object. The entire range of wavelengths cannot be practically scanned, therefore Dozier (1981), developed a technique to compare wavelengths detected in the MIR and TIR ranges. At normal temperatures, background emission in the TIR range is greater than in the MIR range, however, as temperature increases, spectral radiance in the MIR range increases significantly more than in the TIR range as seen in Figure 1. Satellite remote sensing uses this inversion to detect extreme heat and map wildfires (Jones et al., 2017).

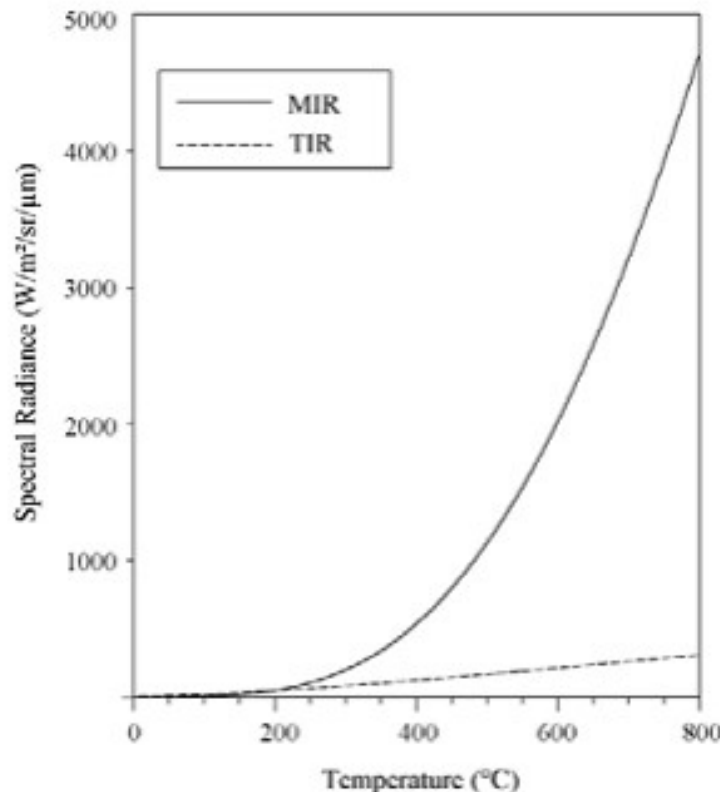


Figure 1 - Relationship between emitted spectral radiance and emitted temperature for the MIR and TIR spectral bands (Jones et al., 2017)

There are some major limitations to satellite bushfire detection. Due to cost limitations, satellites designed for bushfire detection are uncommon. Therefore, satellite bushfire detection is largely done using satellites designed for other purposes. This introduces limitations particularly regarding spatial and time resolution (Martin et al., 1999). Satellites with low spatial resolution are unable to offer accurate fire mapping while low time resolution means they are unable to detect fires early. Thermal sensitivity can also hinder fire detection capabilities. For example, the Advanced Very-High-Resolution Radiometer (AVHRR), is commonly used in satellites for monitoring cloud cover, vegetation cover etc. Channel 3 (3.55-3.93 μ m) of the AVHRR is well suited to fire detection since it is located near peak radiation emittance of object at 800K. However, since it was not designed to detect fires, its saturation temperature is about 47°C. Therefore, hot surfaces which exceed this temperature can often be confused as fires (Martin et al., 1999).

The Moderate Resolution Imaging Spectroradiometer (MODIS) was developed with a significantly higher saturation temperature which improves its performance; however, it still

suffers from other drawbacks of satellite fire detection (Li et al., 2001). The main issue for this method is cloud cover. Thick clouds mask even high intensity fires, while thin clouds can prevent smaller fires from being detected or cause false detection when algorithms attempt to account for cloud coverage (Martin et al., 1999).

An experiment by Csiszer et al. (2006), to validate the use of MODIS for active fire detection found that even fires up to 400, 30-m Advanced Spaceborne Thermal Emission and Reflection Radiometer (ASTER) had less than a 90% probability of being detected. A more recent study by Giglio et al. (2016), corroborated these findings, showing that even with modern algorithms, MODIS still has only a 95% probability of detecting large fires. The probability substantially decreases with smaller fires. Furthermore, these satellite detection methods struggle to detect fires early, before they grow to a size which is difficult to extinguish or even control (Yu et al., 2005).

2.2.2 Wireless Sensor Networks

Wireless sensor networks are networks consisting of a base station and a large quantity of sensor nodes. The sensor nodes are spatially dispersed with the aim of gathering data over a large area and transmitting that data to the base station. From there, the data can be uploaded to the internet where it can be accessed remotely.

Yu et al. (2005), developed a WSN for real-time forest fire detection. The network consisted of nodes which measure temperature and humidity, detect smoke, and are equipped with GPS to track their location. These nodes then transmit this information to a cluster header which relays the information to the manager node. The WSN also consisted of some wind sensors to further assist fire detection. This information is collected and analyzed, which produces an accurate, real-time map of any fires in the forest. A schematic of the WSN is shown in Figure 2.

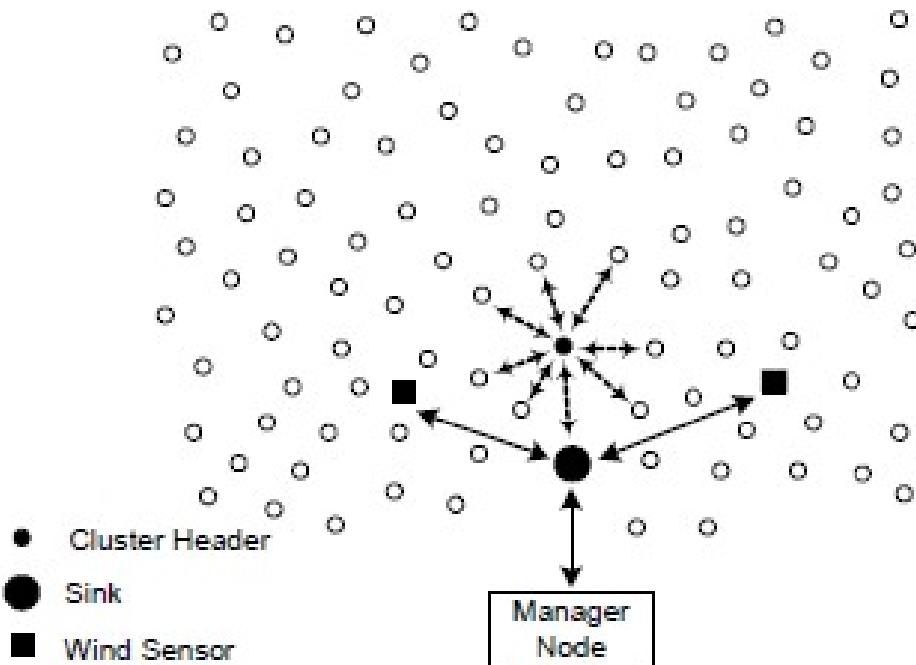


Figure 2 - WSN for real time forest fire detection (Yu et al., 2005)

The major advantage of this method for bushfire detection is that it is not hindered by any external conditions. While cloud cover will decrease the effectiveness of satellite imaging, WSNs will continue to provide accurate, real-time data through all weather conditions. Chaczko and Ahmad's paper (2005), corroborates these findings. Furthermore, the paper demonstrates that these networks can act as mesh topology communication networks. With

the use of commercial wireless transceiver technology, the nodes can send signals to each other and relay that information onto the base station. This essentially means the network can be spread out across a large distance without any issues transmitting data to the base station. Dampage et al. (2022), designed a WSN with machine learning for forest fire detection. The study found that the node could accurately detect 100% of the 22 fire-instances tested. This shows that WSNs are an accurate, real-time option for fire detection.

Antunes et al. (2019), conducted an experiment to validate the use of networked nodes with Infrared (IR) sensors to detect wildfires. The experiment used LoRa technology to wirelessly transmit data detected by the IR sensor when a fire was detected. The IR sensors, denoted by S, detected the fires before transmitting that signal via a wire to the master node. The master node then relays the information forward via wireless communication. The process is seen in Figure 3. The IR sensors accurately detected fires in real-time and the LoRa (long-range) shield was able to transmit that data to the base station. The report, however, highlighted the issue with WSN nodes requiring constant power. Although low power technologies like LoRa reduce the power usage of the nodes, batteries cannot last extended periods of time while powering sensors and transmitting data.

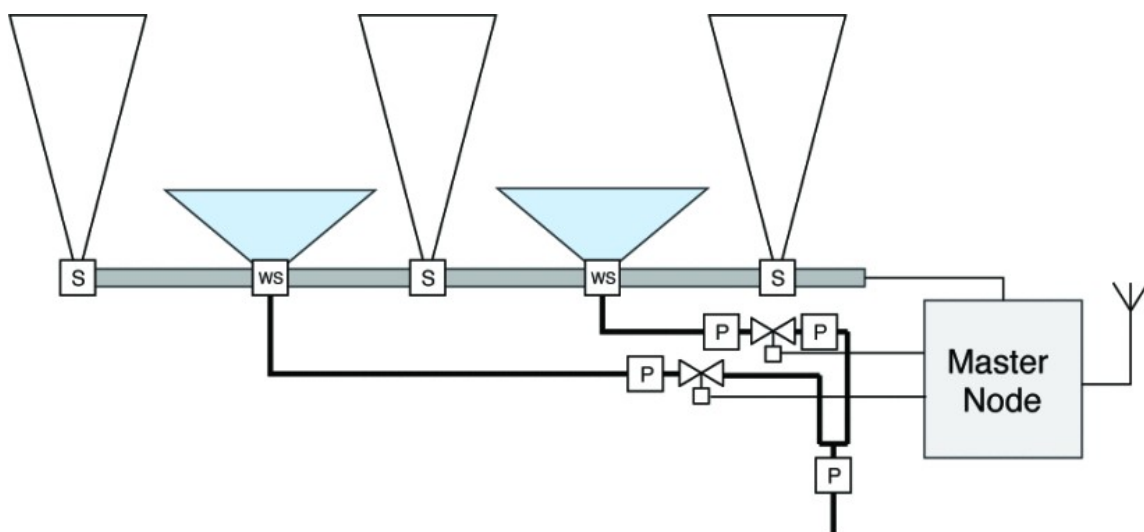


Figure 3 - Wireless Sensor Node Schematic for Experiment by Antunes et al. (2019)

Mayer et al. (2019), developed a LoRa smart sensor node which operated in a deep sleep, only using significant power every 10-minute interval to use the sensors. Even with this design, a 2000mAh battery could last up to 4.5 years under ideal conditions. This method also means that the WSN could have up to a 10-minute delay in detecting fires, which negates its most desirable trait of being a real-time solution.

While WSNs offer the most accurate and time efficient detection of bushfires, they suffer from the fact that each node requires an individual power source. Solar powered nodes are not an option given the environment the nodes are used in does not offer any significant sunlight. Therefore, these systems require tedious maintenance which makes them currently less desirable than satellite detection. There is a clear research gap for an early bushfire detection system with the accuracy of WSNs, without the drawback of the power requirements. A near zero-power wireless sensor node with LoRa communication would fill this gap.

2.3 LoRaWAN

Low-Power Wide Area Networks (LPWAN) is a category of wireless communication technologies with low power consumption. These technologies offer communication upwards of several kilometers, with a single gateway being able to demodulate signals sent from thousands of devices or nodes (Casals et al., 2017). LoRa is one of these LPWAN technologies. It operates on ISM bands, capable of transmitting long range signals with low power consumption. LoRaWAN is the wide area network protocol based on LoRa. A LoRaWAN system is shown in Figure 4, where the end-devices or nodes can transmit to the gateways or base stations which can then upload to the network. The figure also demonstrates the bidirectional capabilities of LoRaWAN as a message can also be sent to the gateway from the network and passed on to the node.

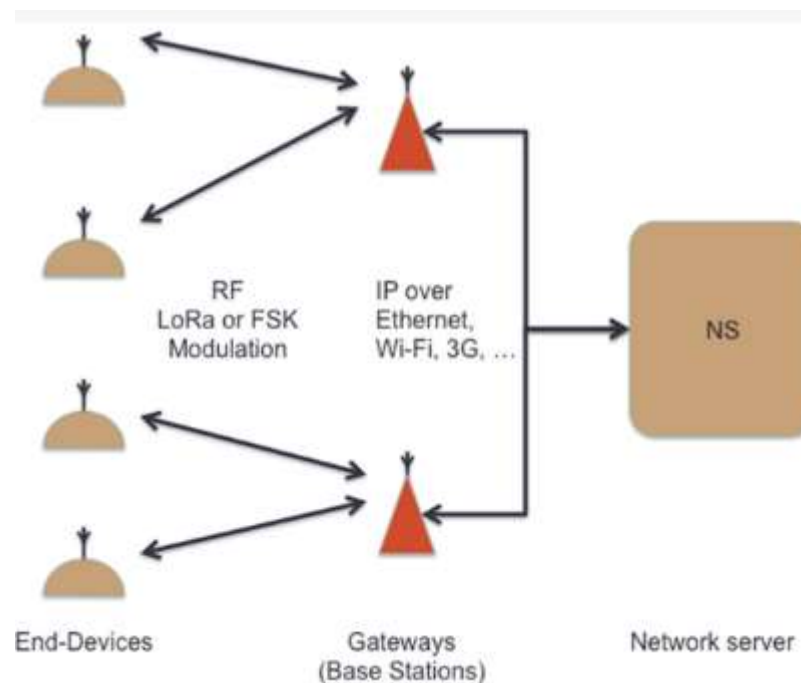


Figure 4 - LoRaWAN System Flowchart (Casals et al., 2017)

Wi-Fi is currently the most popular technology for wireless communication; however, the power usage of Wi-Fi is significantly higher than LoRa, while offering much lower range which makes it a poor option for use in WSNs as seen in Figure 5. Zigbee offers a low power solution for high data rate transfers, however, its range is limited to 10 to 100 meters compared to several kilometers with LoRa which limits its usefulness (Devalal and Karthikeyan, 2018).

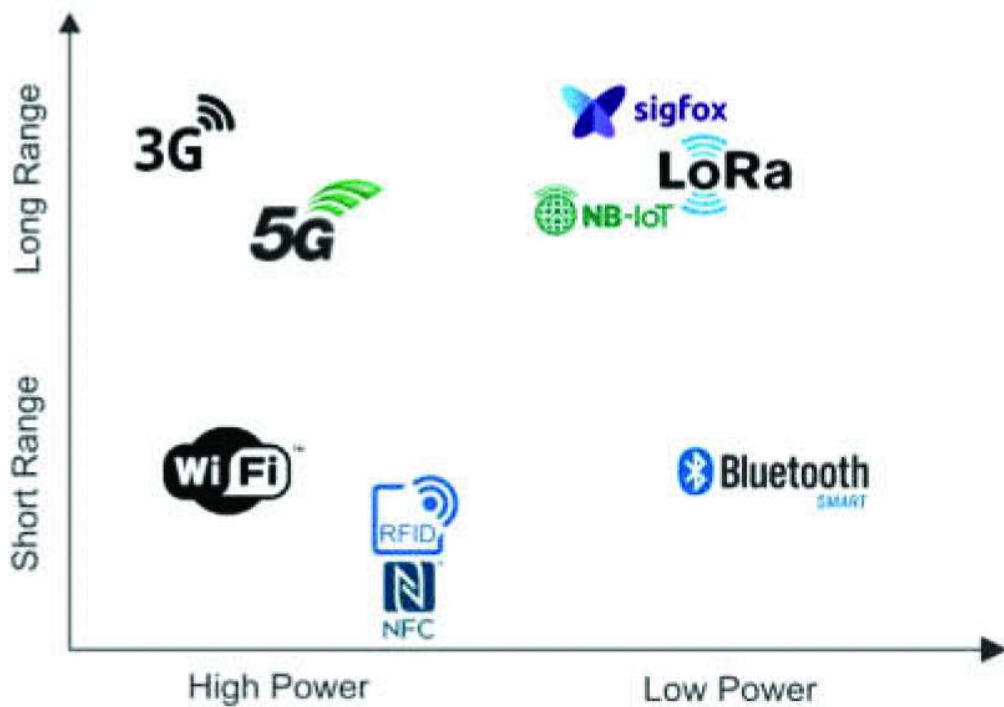


Figure 5 - Summary of Communication Technologies (Mayer et al., 2019)

Other LPWAN technologies including Sigfox, NB-IoT are competing options for WSNs as they offer low power, long-range communication, like LoRa. Hossain and Markendahl (2021), conducted an experiment, comparing the cost of LPWAN technologies. The report found that LoRa was cheaper than both Sigfox and NB-IoT for 3 out of 4 scenarios. It found that where data rate requirements were not high, LoRa was the most cost-effective solution. Devalal and Karthikeyan (2018), corroborates these findings, mentioning that NB-IoT is well suited to high latency or high data rate, while LoRa is most suited to lower data rate uses. As WSNs used for fire detection only require a low data rate to transfer temperature, humidity, and smoke readings etc. LoRa is the most well suited LPWAN technology for these networks.

2.4 Zero-Power Switch

For WSNs to be a viable option for early bushfire detection, the need for maintenance due to individual nodes requiring power supply should be addressed. One solution to this issue is the use of a zero-power switch. These switches are usually open, but close the electrical circuit when data of importance, in this case high temperatures, is detected. This would allow these WSN nodes to use zero-power prior to a fire being detected.

The use of micro electromechanical systems (MEMS) switches in low voltage circuits, takes advantage of the piezoelectric effect. The switch is designed that when an actuation voltage is applied, a downward force results, causing the switch to close and complete the circuit (Jaafar et al., 2014). This process is shown in Figure 6 and Figure 7.

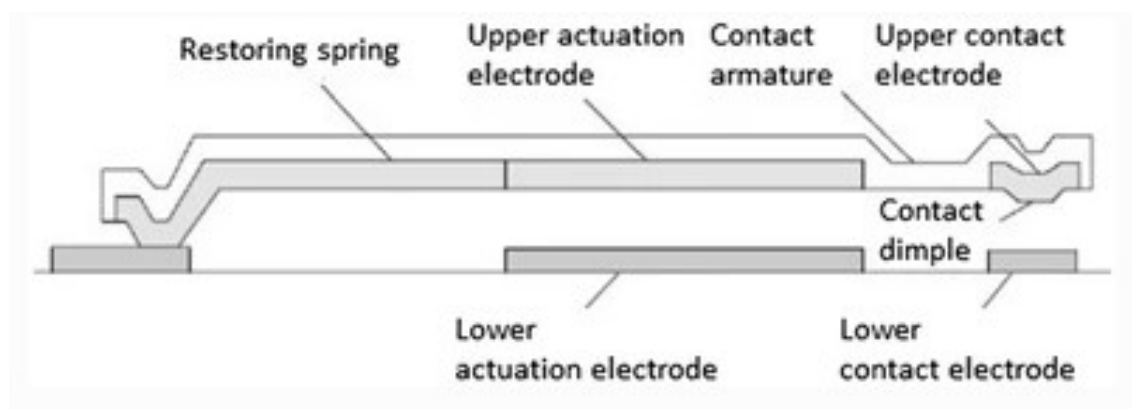


Figure 6 - MEMS Switch in OFF State (Jaafar et al., 2014)

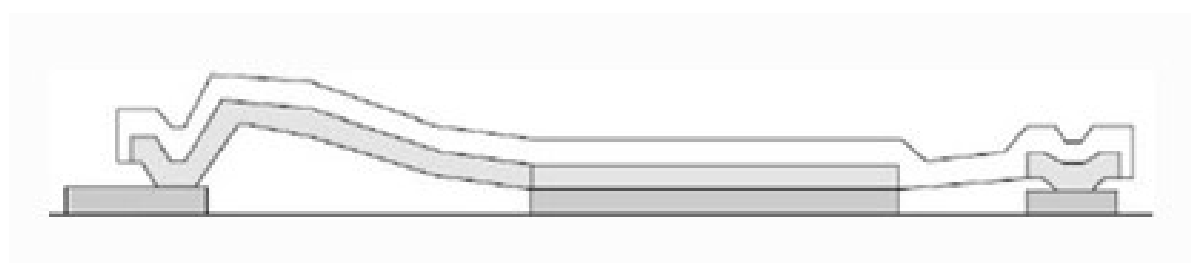


Figure 7 - MEMS Switch in ON State (Jaafar et al., 2014)

The electrostatic actuation of MEMS switches requires high voltage; however, it does not consume any current. Therefore, MEMS switches cause very low power dissipation (10 – 100nJ). These switches are often expensive due to the need for packaging and a high-voltage drive chip (Rebeiz, 2003).

Rajaram et al. (2018), designed a wireless sensor node using a MEMS switch for near-zero power consumption and an IR sensor to detect fires. This report found that the node used just 2.6nW of power while the switch was in the open state.

A thermal MEMS switch has a thermal actuator which is forced upwards when the actuation voltage is applied as seen in Figure 8. Prior to actuation voltage, the circuit is incomplete (left), but when the voltage is applied, the actuator closes the circuit (right).

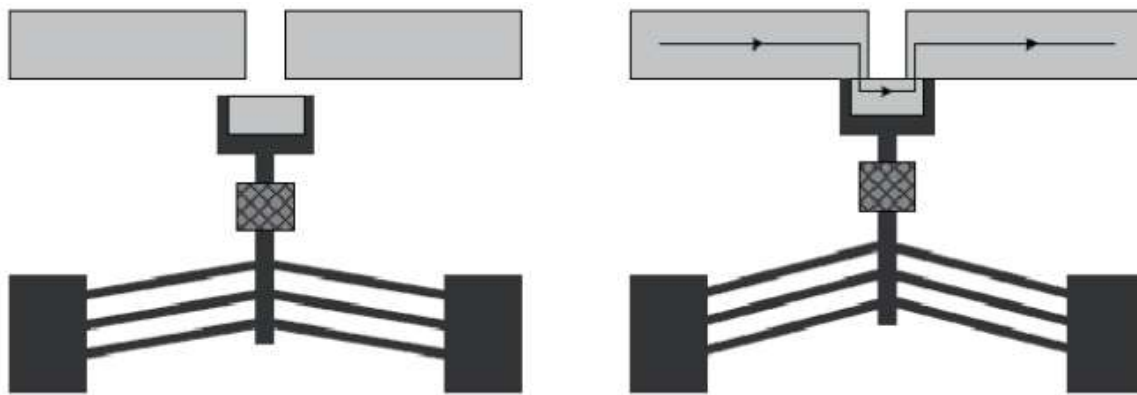


Figure 8 - Thermal Actuated MEMS Switch (Li et al., 2010)

Thermal mechanical switches utilize mechanical movement to close the circuit. As materials are heated, their properties alter, of interest in this case is thermal expansion. These switches make use of this principle to close a circuit when a temperature is measurably high. This allows the switch to remain open while no data of significance is detected. These switches are cheaper and can offer zero power consumption when open compared to very low power leakage with MEMS.

2.5 Summary

This literature review analysed satellite-based wildfire detection and found that, while it was a very effective solution under normal conditions, cloud cover and hot surfaces made it only 90-95% effective at detecting even large fires. The method also does not provide real-time detection and often alerts authorities too late to control the fire.

Wireless sensor networks were then reviewed to offer a solution which provides early detection and is not limited by weather conditions. It was found that this method is effective at accurately detecting fires during their early stages. The drawback of WSNs however, was that each individual node requires a power supply. This introduces tedious maintenance which greatly increases its expense and manpower requirement.

Based on this review, a research gap of a near zero-power wireless sensor node was identified. To fill this research gap, a wireless sensor node with low power, long range communication that consumes no power prior to a fire event must be designed. Therefore, Low Power Wide Area Networks (LPWAN) were researched to find a suitable option for WSNs. It was found that LoRa offered the most cost-efficient solution for this case. Thermal switches were also researched, focusing on thermal mechanical switches including MEMS switches. It was established that this technology could offer a potential solution to a near zero-power node.

Therefore, the aim of this project is to fill the research gap of a near zero-power wireless sensor node by designing and validating a node using LoRa and a thermal mechanical switch.

3 METHODOLOGY

3.1 Design Process

The first step in the design process was to select adequate parts for the sensor node. As mentioned in the literature review of this report, LoRaWAN offers the best performance low power, long range communication which is suitable for the application of this device. An Arduino compatible LoRa shield (Duinotech XC4392) was paired with an Arduino Uno as the node. The gateway selected is the Duinotech XC4394. The circuit of the design is shown in Figure 9, while the switch is open, no link is established between the node and gateway.

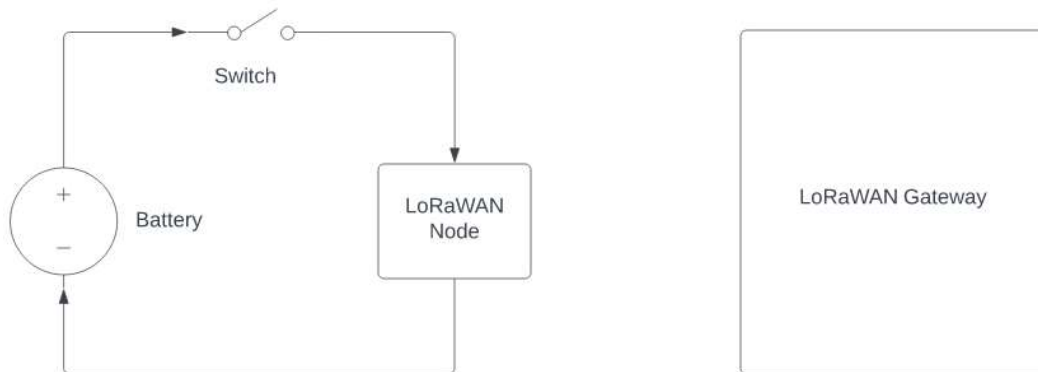


Figure 9 - Zero Power WSN Design

It was also discussed that advanced technology such as MEMS switches are more expensive than basic thermal mechanical switches. Since the device has no need for the added benefits of a MEMS switch, a basic thermal mechanical switch is used to reduce the cost of the node while fulfilling the purpose of near zero-power usage. A 9-volt battery is then connected to the LoRa shield via the mechanical switch as seen in Figure 10. This allows the node to draw no power until the switch reaches its thermal trip temperature. When the switch closes, the shield transmits a modulated signal over the ISM band.

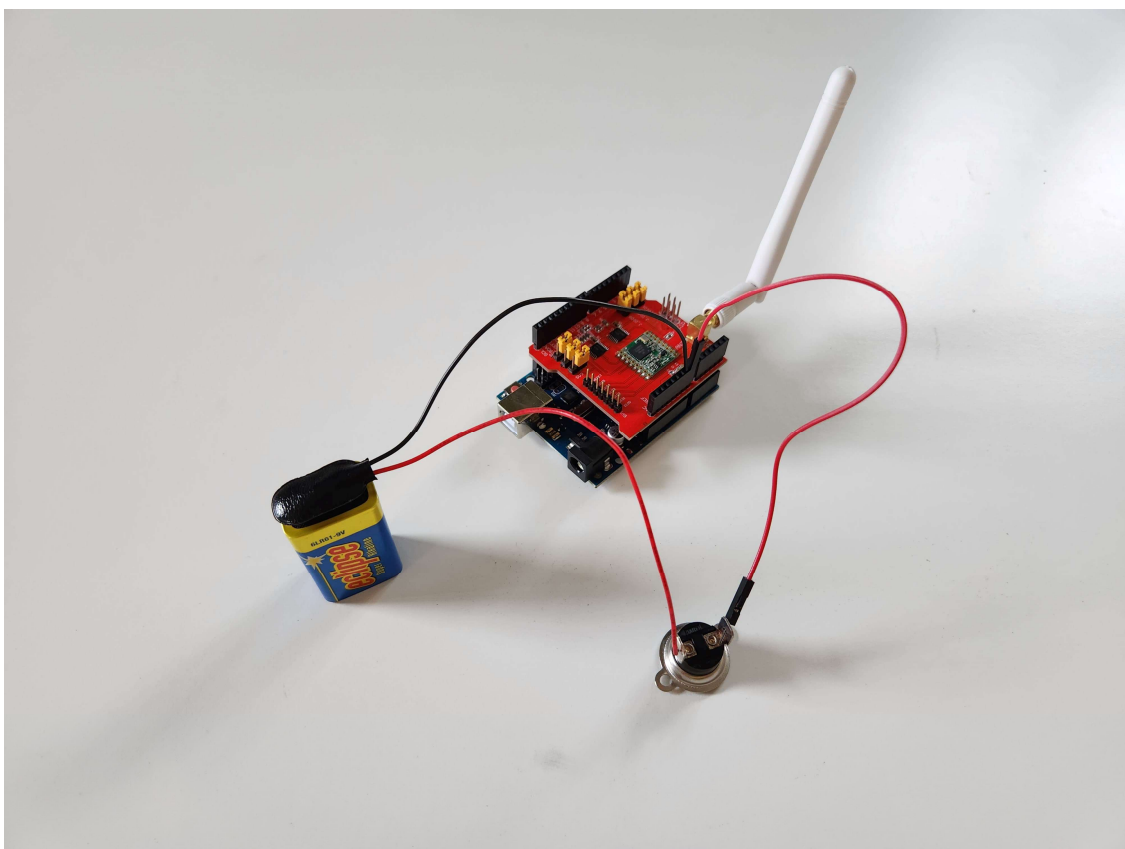


Figure 10 - LoRaWAN Node with Thermal Mechanical Switch

The LoRaWAN gateway, connected to a laptop via Wi-Fi, then demodulates the signal, displaying the information on the laptop. This data can then be uploaded to the cloud, making it accessible remotely. LoRaWAN gateways are capable of handling 100's of nodes simultaneously, however, as this investigation aims to prove the concept, only 1 node is used. The entire process of the node transmitting a signal which is demodulated by the gateway and displayed on a laptop is seen Figure 11 where the laptop screen displays the message received from the node.

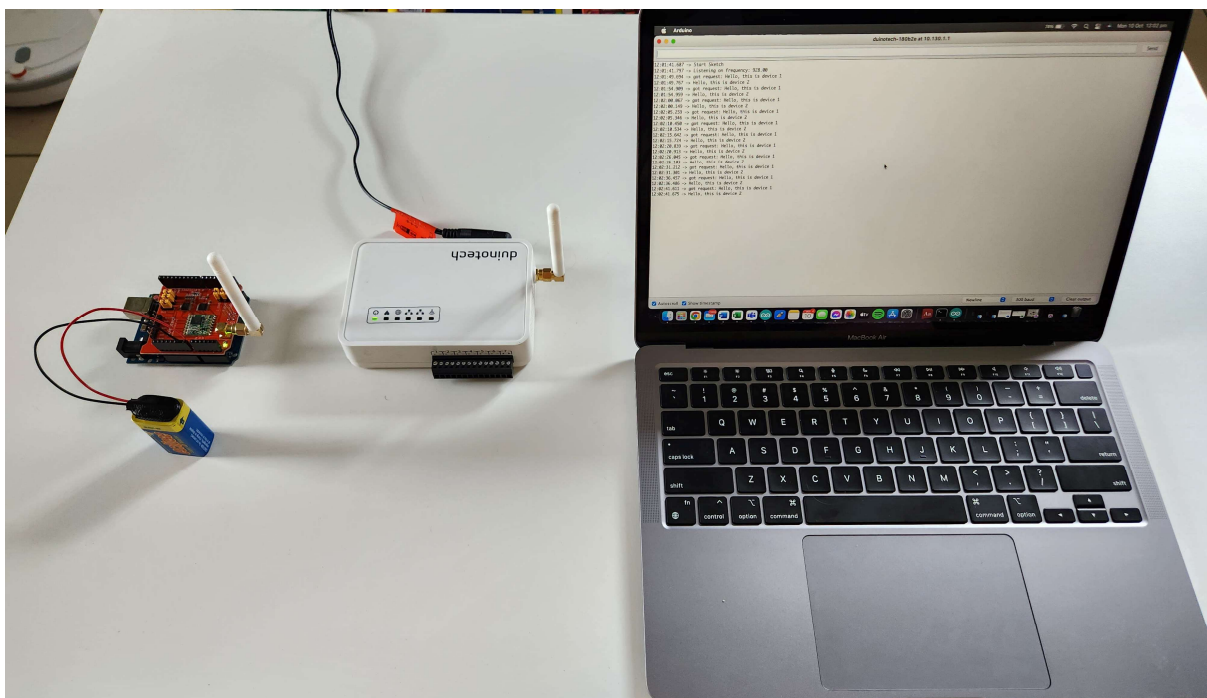


Figure 11 - LoRaWAN Node Signal Demodulated by Gateway and Displayed on Laptop

3.2 LoRaWAN Experimental

In the literature review of this thesis, it was identified that LoRaWAN signal performance varies based on the environment and landscape. For example, Vatcharatiansakul et al. (2017) conducted an experiment which showed a LoRaWAN node able to transmit a signal up to 2km outdoors but only up to 120 meters indoors. Therefore, this thesis aims to investigate the performance of the node in a range of environments. It will compare free space (line of sight), urban, and bush performance. The goal of these comparisons is to evaluate the validity of the device for its intended use.

For testing in each environment, the node will be setup as in Figure 11. The gateway will also be setup as in Figure 11 for the urban test. However, for the free space and bush tests, as the gateway requires remote power, it will be setup as seen in Figure 12. For these tests, the gateway is powered using a 12-volt car battery and is places on the roof of the car to minimize any unwanted obstructions from immediate surrounding environment.



Figure 12 - Gateway Powered from Car Battery

The first environment tested will be free space, where no buildings or environment should obstruct the signal as seen in Figure 13. The testing location allows for a maximum distance of 800 meters where line of sight is maintained. The node will begin directly next to the gateway, received signal strength indicator (RSSI) and signal-to-noise ratio (SNR) will be measured 3 times. This procedure will be repeated every 25 meters until either 800 meters or the node's signal fails to reach the gateway.

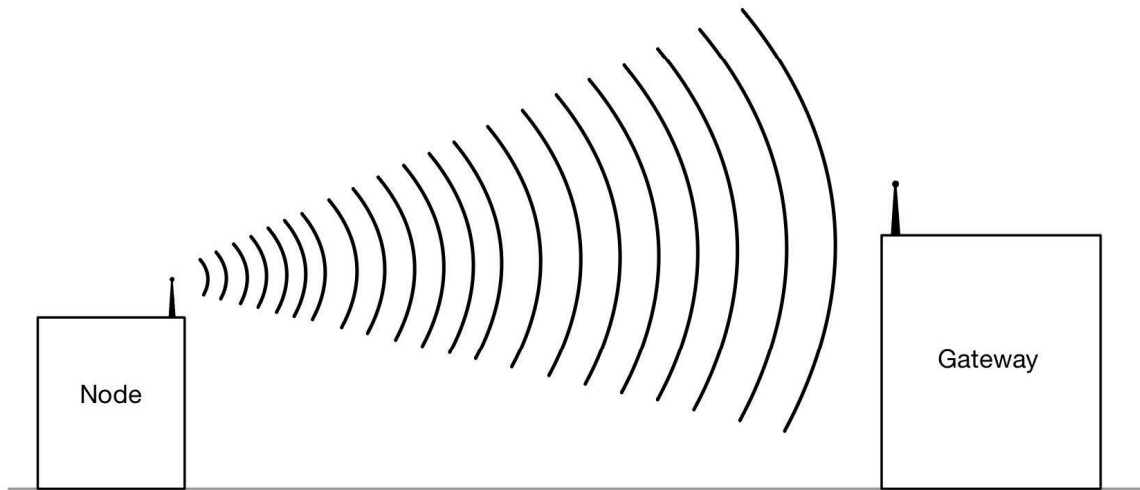


Figure 13 - Free Space Test Schematic

The second environment tested will be urban area, where buildings should obstruct the signal as seen in Figure 14. The procedure for this test is the same as with the free space, however, the node will be placed in various, random locations to allow for data with varying levels of buildings obstructing the signal.



Figure 14 - Urban Test Schematic

The final environment tested will be bush where a forest environment should obstruct the signal as seen in Figure 15. The maximum straight distance covered by bush in this location is 350 meters. The procedure is similar to previous tests; however, the node and gateway will be placed on opposite sides of the bush-covered area. Data will be gathered each 25 meters until either 350 meters or the node's signal fails to reach the gateway.

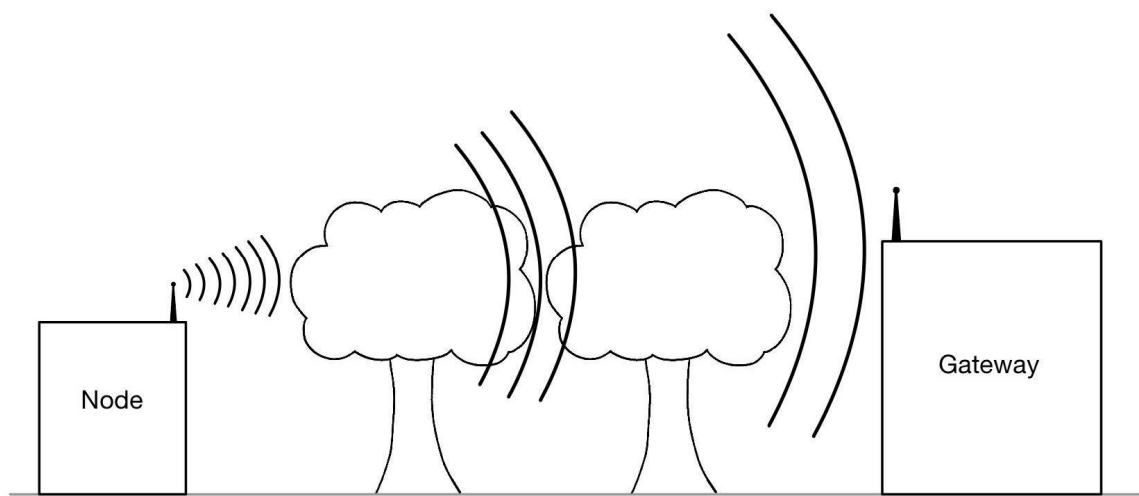


Figure 15 - Bush Test Schematic

Once all tests have been completed, RSSI and SNR data for each environment will be graphed over distance. Analysis of this data will compare LoRaWAN performance based on environmental factors, and the magnitude of the effect of obstacles such as buildings and trees will be ranked. These results will be compared with established data to evaluate the validity of LoRaWAN for this use case. Performance of the device with regards to the antenna will also be discussed, to determine whether this device is adequate for the task, or a high gain antenna is required for transmitting through heavy bush.

3.3 Thermal Mechanical Switch Experiment

After testing and discussing LoRaWAN performance, the switch will be tested. The purpose of the switch is to use no power while no fire is present. Once the switch detects high heat, indicating a fire, it closes the circuit, which then allows the LoRaWAN shield to transmit a signal to the gateway. The working principle of the switch is shown in Figure 16. When no heat is applied, the circuit remains open. However, when the switch is heated it causes the mechanical deformation in the form of bending, this causes the switch to close which completes the circuit.

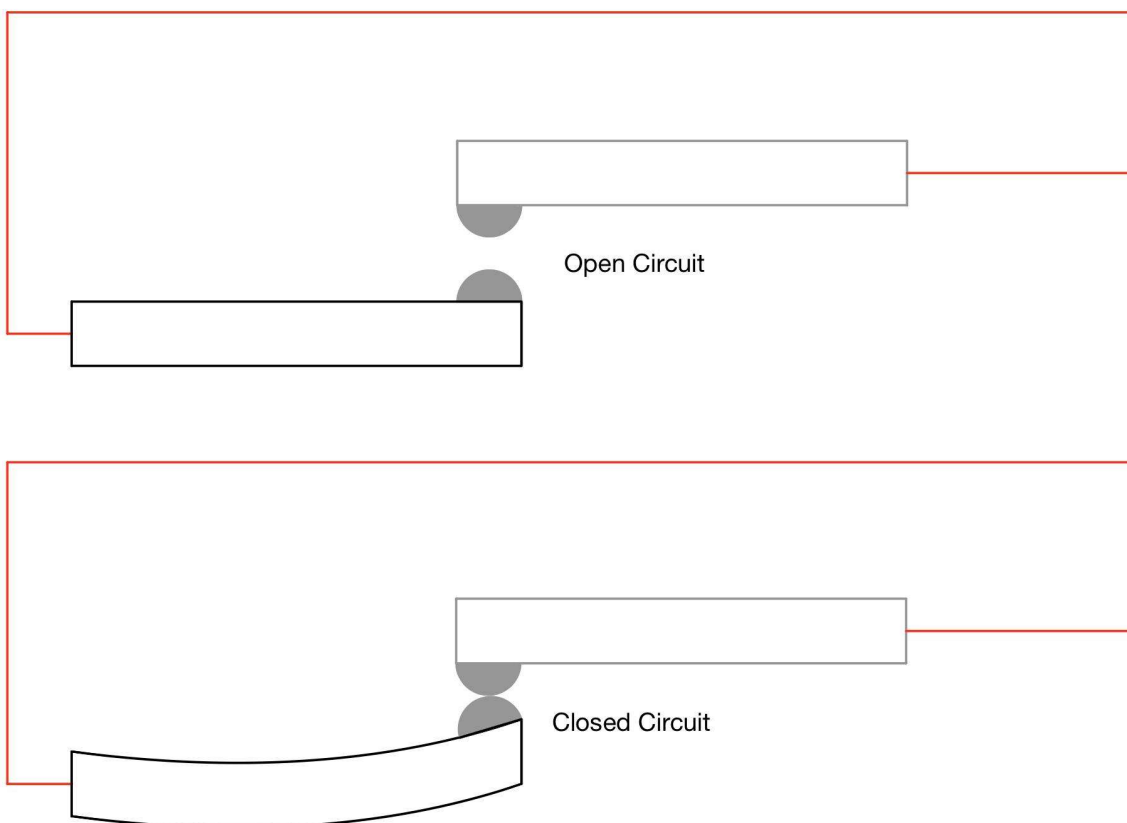


Figure 16 - Working Principle of Thermal Mechanical Switch

There are three main aspects of the switch which will be tested:

- Power usage while the switch is open and closed
- Time taken for the switch to close
- Validation that the signal from the node will be sent to the gateway in the event of a fire.

For all 3 tests, the process will be repeated on both a 70-degree and a 100-degree switch. For testing power usage and validating the device, the use of 2 switches offers corroboration of results. When testing the time taken for the switch to close, the use of the 2 switches will offer insight into the ideal thermal trip temperature. As the device cannot withstand extreme heat for an extended duration, the switch needs to close quickly so that the node can send a signal before it is damaged in the fire. However, the trip temperature needs to also be hot enough that it will not close due to hot temperatures not caused by a fire.

The power usage of the device is tested to validate the zero-power usage claim while no fire is present. It will also offer insight into how long a node could operate without a thermal mechanical switch to evaluate the advantage of its use. A multimeter will be used to measure the voltage (V) and the current (I) in the circuit both while the switch is open and closed. Power consumption (P) can then be calculated using Equation 1.

$$P = V \times I \quad (1)$$

To measure voltage, the multimeter is placed in the circuit in parallel as seen in Figure 17.

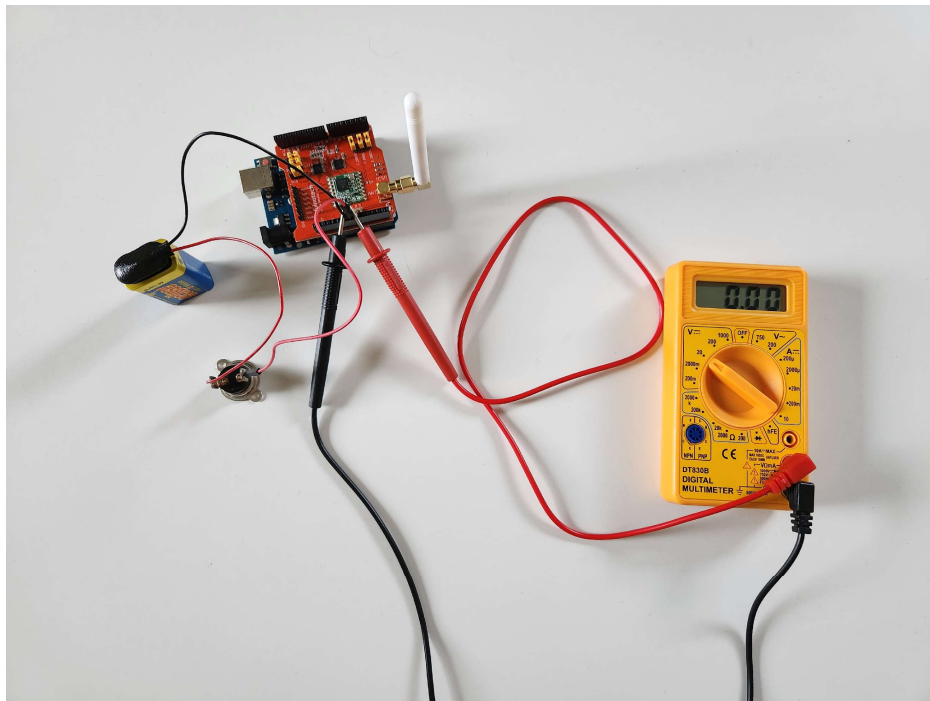


Figure 17 - LoRaWAN Node Circuit with Multimeter in Parallel

To measure, the current, the multimeter is placed in the circuit in series as seen in Figure 18.

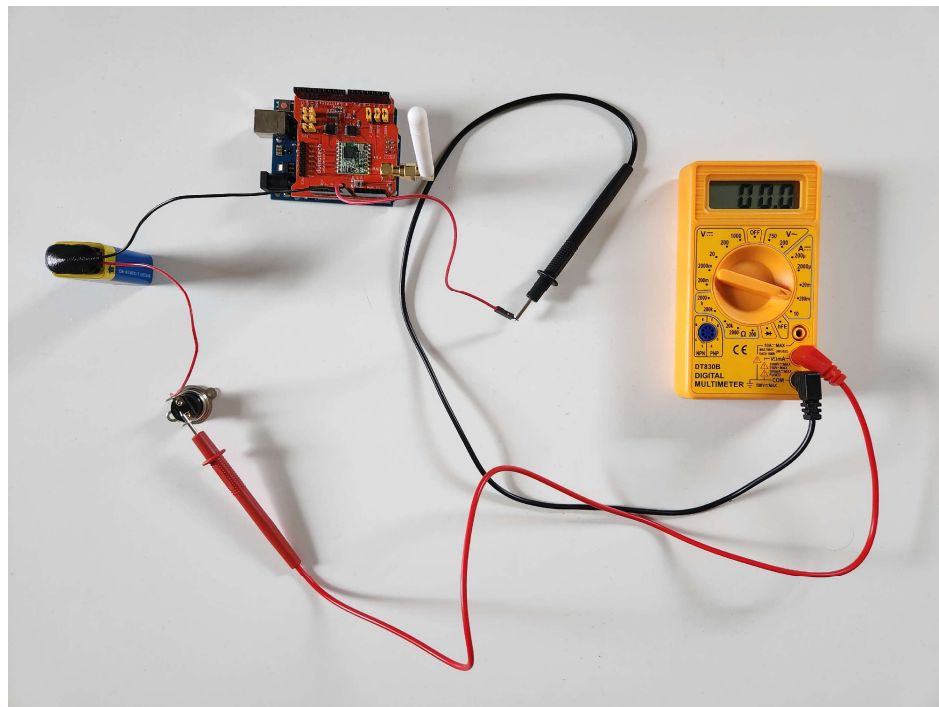


Figure 18 - LoRaWAN Node Circuit with Multimeter in Series

To measure the time taken for the switch to close, a multimeter is connected to the device in series like in Figure 18. The device is placed on a table outside with no surrounding buildings or trees to remove any risk of causing a fire. The switch is then held above a lighter using tongs to reduce risk of burns to skin. The lighter is then turned on at the same time as a stopwatch is started. The setup of this test is shown in Figure 19. When the multimeter shows a change in current, indicating that the switch has closed, the stopwatch is stopped, and the time is recorded.

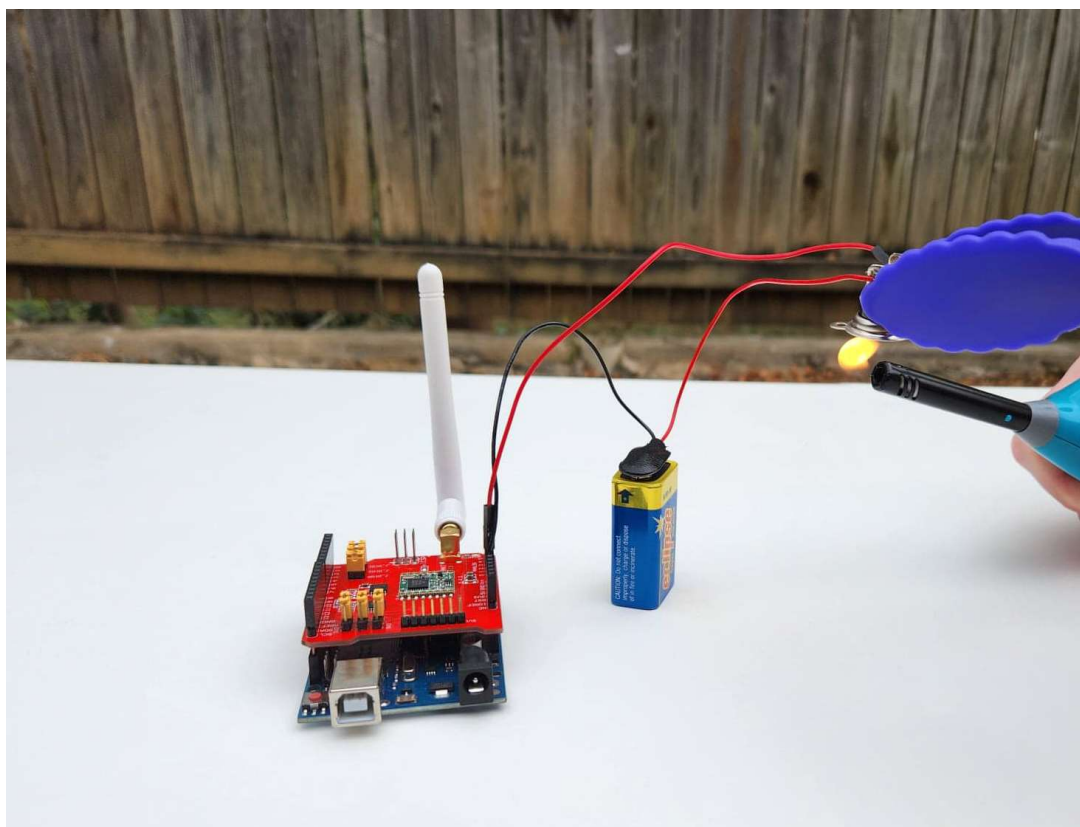


Figure 19 - Thermal Mechanical Switch Experimental Setup

To validate that the node will send a signal to the gateway due to a fire, the node is constructed like in Figure 19, and the gateway is connected to the laptop. Arduino IDE is open on the laptop, which displays any signals received by the gateway. The gateway should not display any received signals while the lighter is not turned on and the switch is open like in Figure 20. When the lighter is turned on, the switch should close, and the node should send a signal which will appear on the laptop.



Figure 20 - Gateway Listening for Signal from Node

The results of these three tests will then be used to discuss the validity of this thermal mechanical switch's use in the LoRaWAN node. The time for the switch to close will be used to discuss what thermal trip temperature is ideal for the node. The power consumption will be used to both validate the zero-power usage when the switch is open and to discuss the advantages of using the switch as opposed to other solutions.

4 EXPERIMENTAL RESULTS

4.1 LoRaWAN Distance Testing

In wireless communication, a receiver's ability to demodulate a signal depends on the received signal strength (RSSI) and the signal-to-noise ratio (SNR). RSSI is a measurement of the signal strength and is measured in decibels per milliwatt (dBm). The closer the RSSI is to 0dBm, the stronger the received signal (Rahman et al., 2018). Typically, a LoRaWAN RSSI value of -30dBm indicates a strong signal, while a value of -120dBm indicates a weak signal. RSSI mainly diminishes due to path loss over distance as seen in Figure 21. SNR is a ratio of the received signal power to the noise floor and is measured in decibels (dB). Where the received signal is above the noise floor, SNR is positive and where it is below, SNR is negative. LoRa can demodulate signals up to 20dB below the noise floor, however, typically an SNR of -10dB or lower indicates a poor-quality signal (Rahman et al., 2018).

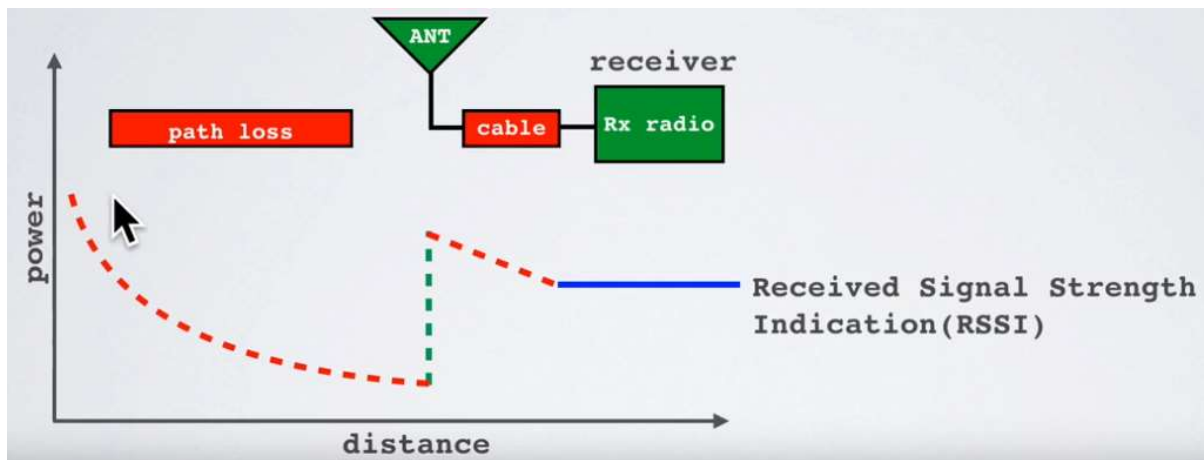


Figure 21 - Signal Power over Distance (Eric, 2018)

4.1.1 Free Space (Line of Sight) Test

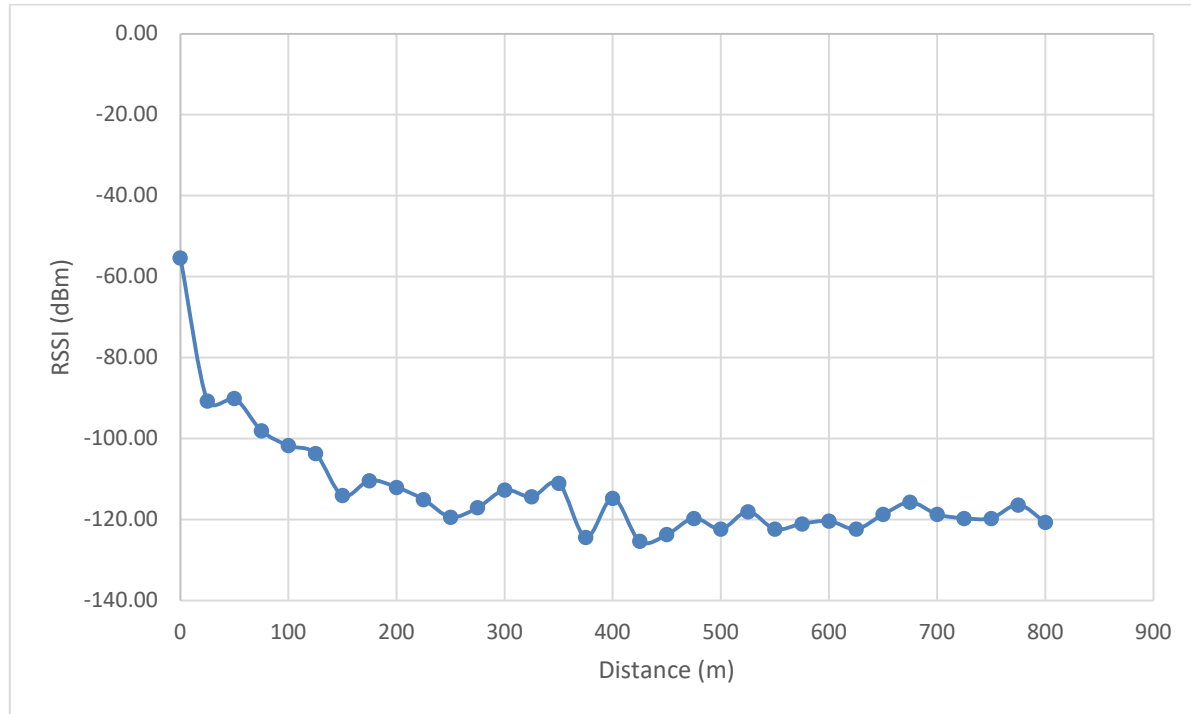


Figure 22 - RSSI over Distance for Free Space Test

Figure 22 shows the received signal strength indicator of the LoRaWAN signal plotted against distance for the free space test. At 0 meters RSSI is -55.33dBm, over the first 25 meters it decreases to -90.67dBm and by 250 meters it is down to -119.33dBm where it remains reasonably constant until 800 meters. After 800 meters, no tests were done due to space limitations.

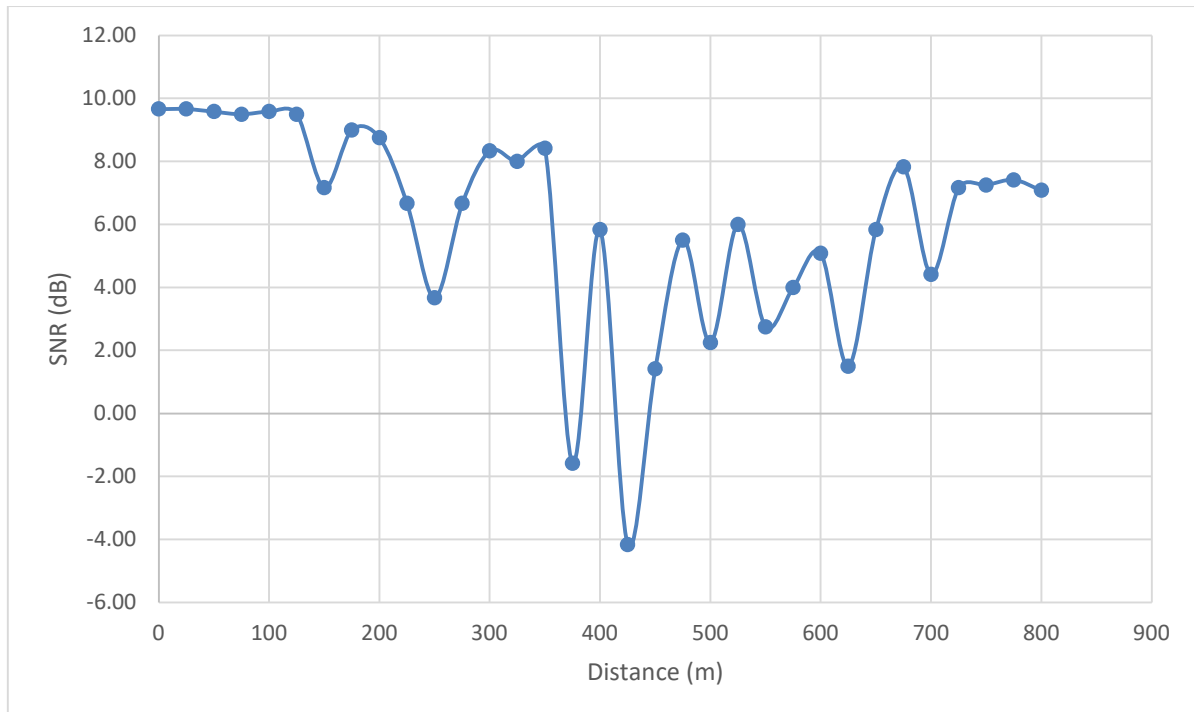
**Figure 23 - SNR over Distance for Free Space Test**

Figure 23 shows the signal-to-noise ratio of the LoRaWAN signal plotted against distance for the free space test. Over the first 125 meters, the SNR remains between 9dB and 10dB before it drops to 7.17dB at 150 meters. From 150 to 700 meters, the SNR fluctuates significantly between 9dB and -4dB until it regains consistency from 725 to 800 meters at about 7dB. After 800 meters, no tests were done due to space limitations.

4.1.2 Urban Test

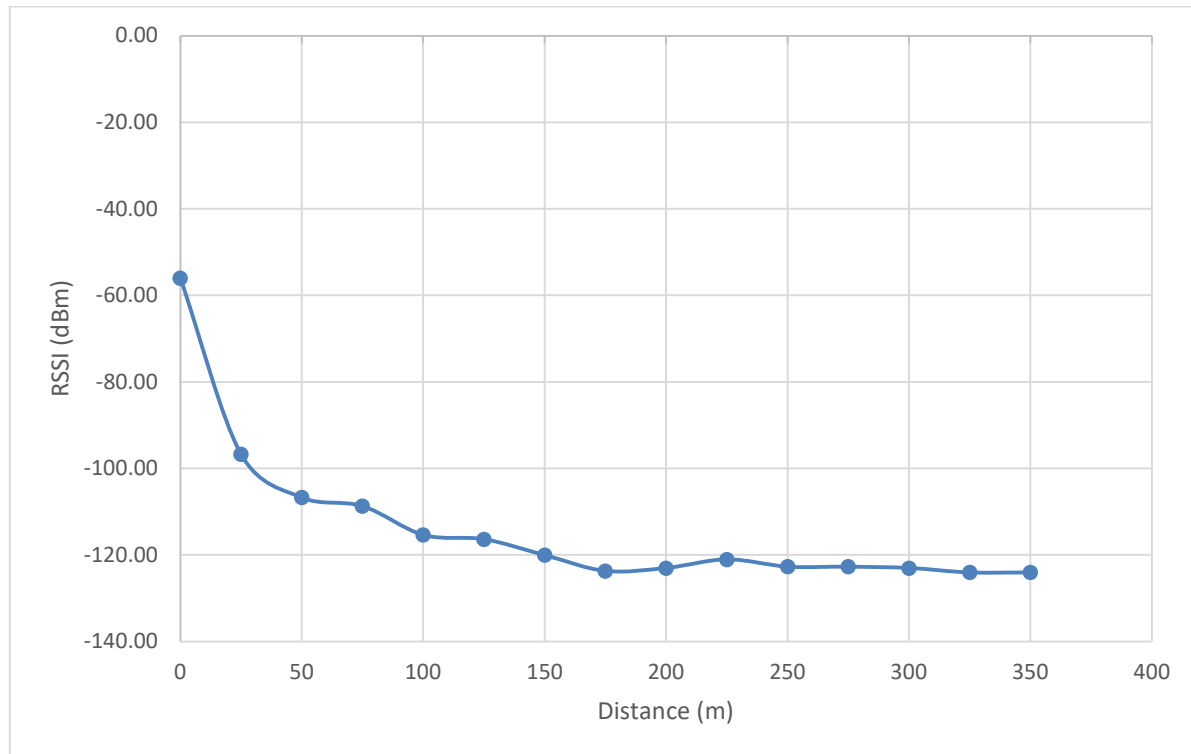


Figure 24 - RSSI over Distance for Urban Test

Figure 24 shows the received signal strength indicator of the LoRaWAN signal plotted against distance for the urban test. At 0 meters RSSI is -56.00dBm, over the first 25 meters it decreases to -96.67dBm and by 150 meters it is down to -120.00dBm where it remains reasonably constant until 350 meters. After 350 meters, the gateway was unable to demodulate the node's signal.

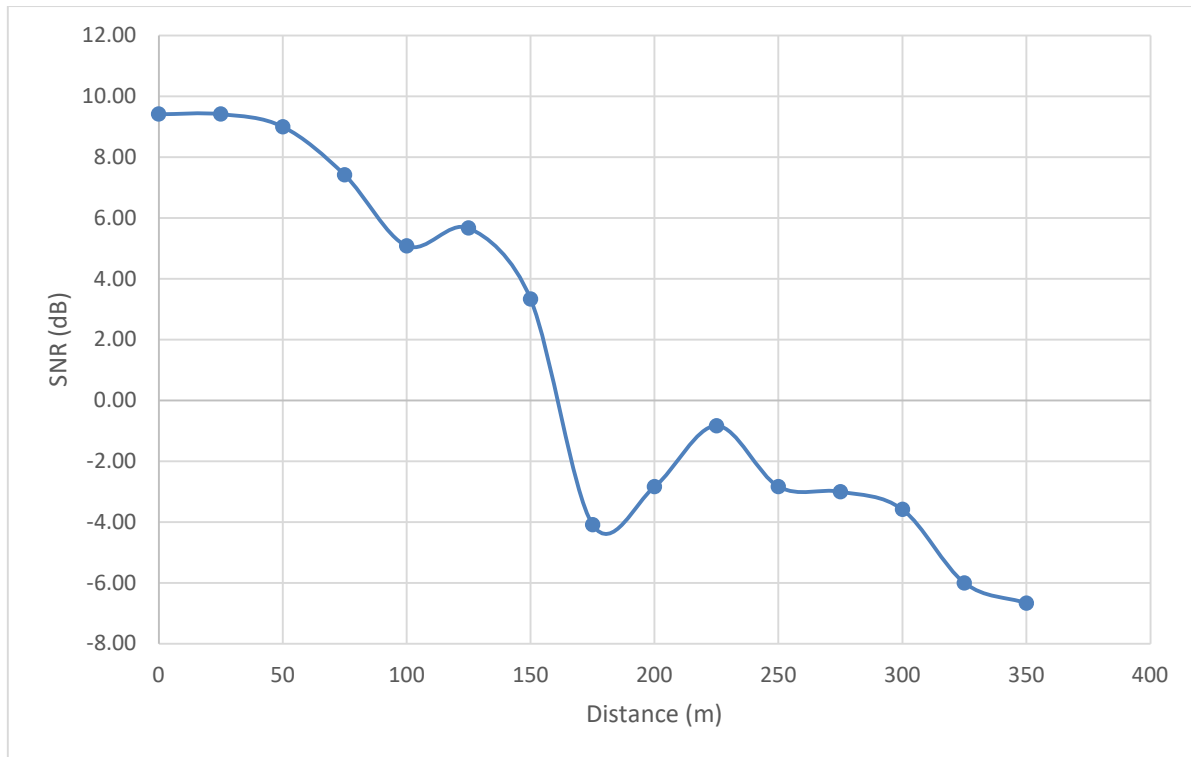


Figure 25 - SNR over Distance for Urban Test

Figure 25 shows the signal-to-noise ratio of the LoRaWAN signal plotted against distance for the urban test. Over the first 50 meters, the SNR remains between 9dB and 10dB before it drops to 7.42dB at 75 meters. SNR continues to drop after 75 meters with the biggest drop being from 150 to 175 meters. After 350 meters, the gateway was unable to demodulate the node's signal.

4.1.3 Bush Test

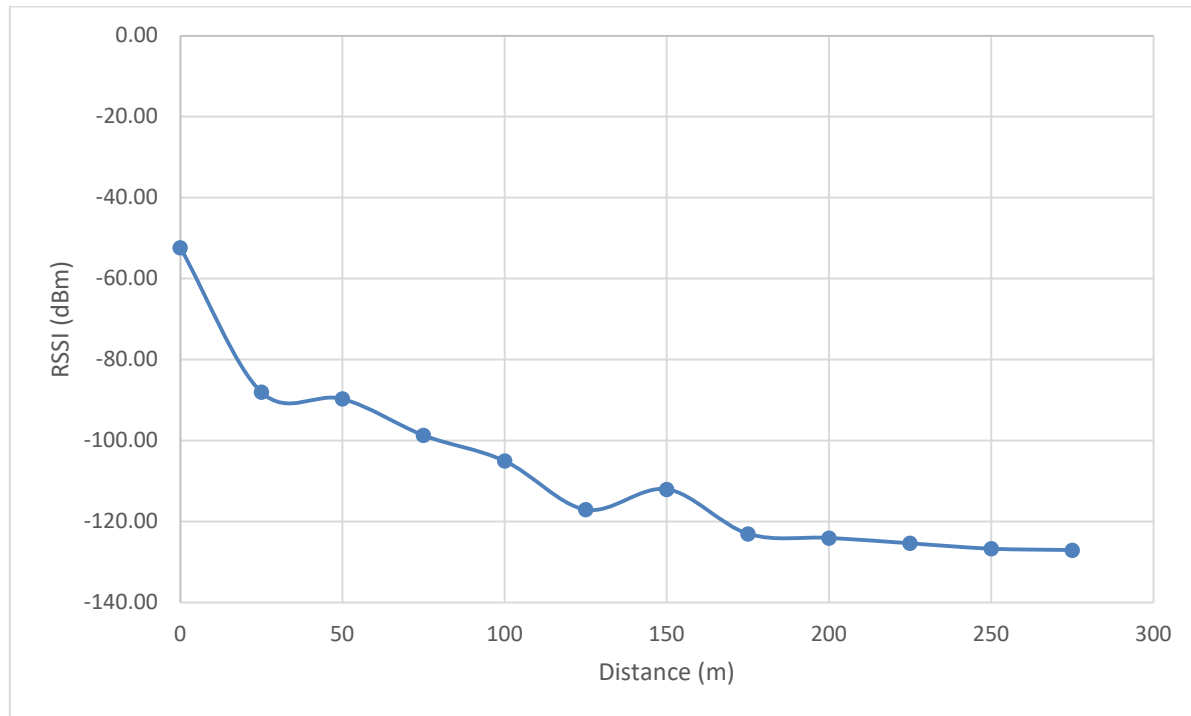


Figure 26 - RSSI over Distance for Bush Test

Figure 26 shows the received signal strength indicator of the LoRaWAN signal plotted against distance for the bush test. At 0 meters RSSI is -52.33dBm, over the first 25 meters it decreases to -88.00dBm. From 25 meters on, it steadily decreases to -127.00dBm at 275 meters, with the exception of an increase of 5dBm between 125 and 150 meters. After 275 meters, the gateway was unable to demodulate the node's signal.

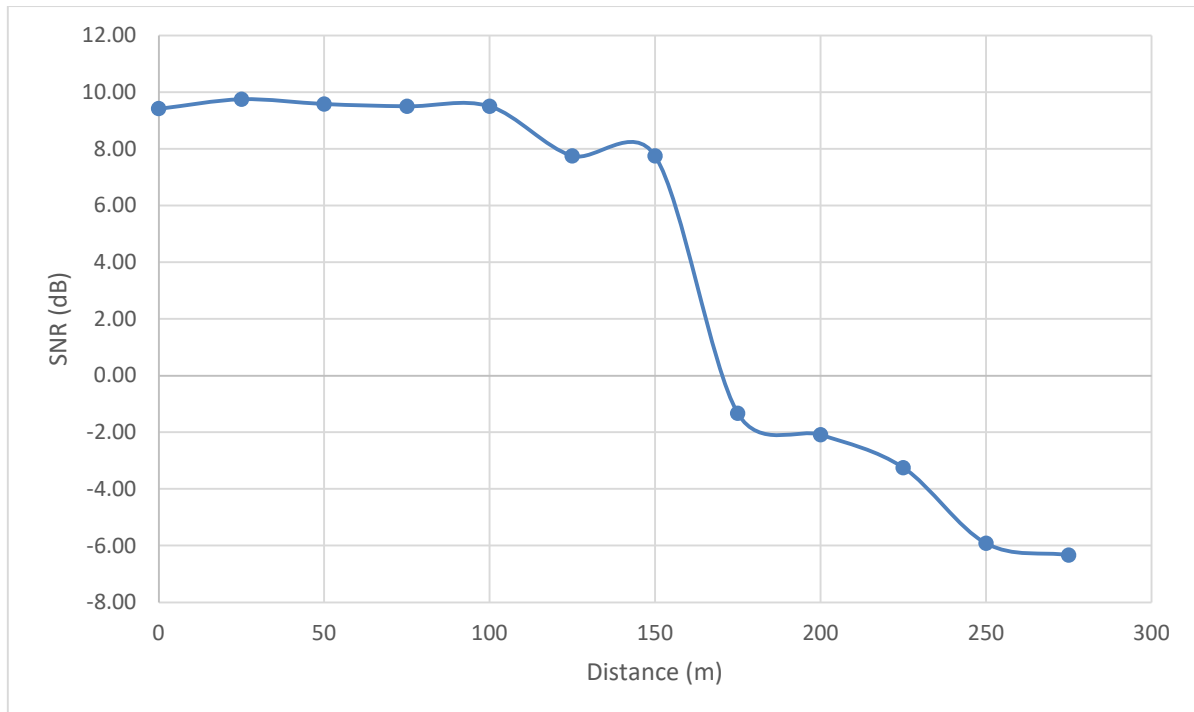


Figure 27 - SNR over Distance for Bush Test

Figure 27 shows the signal-to-noise ratio of the LoRaWAN signal plotted against distance for the bush test. Over the first 100 meters, the SNR remains between 9dB and 10dB before it drops to 7.75dB at 125 meters. From 150 to 175 meters, the SNR drops from 7.75dB to -1.33dB. From 175 to 275 meters, the SNR gradually decreases to -6.33dB. After 350 meters, the gateway was unable to demodulate the node's signal.

4.2 LoRaWAN Discussion

4.2.1 Free Space Test

Figure 28 shows a satellite image of the environment where the free space test was conducted, where the red line shows the path where data points were collected.



Figure 28 - Free Space Test Data Point Map (Google Maps, 2022)

Throughout the 800 meters where the experiment was conducted, line-of-sight is always maintained, however, the elevation is not consistent. Figure 22 shows RSSI plotted against distance for the free space test. The graph shows that the signal strength gradually drops over the first 150 meters before remaining largely constant. Figure 23 shows the SNR plotted against distance for the free space test. In this graph, SNR remains reasonably constant for the first 125 and the last 75 meters of the test. However, throughout the test, SNR shows large fluctuations. This evidence suggests that in an environment where the elevation where a LoRaWAN signal is transmitted from is inconsistent, there will be little to no effect on the received signal strength but will be a significant effect on the signal-to-noise ratio. From the 725-meter to the 800-meter point in the free space test, the ground elevates significantly. These points in Figure 22 and Figure 23 show that RSSI does not increase due to the elevation, but SNR does. This evidence suggests that RSSI mainly depends on the distance

between the node and the gateway, while SNR also depends on the elevation difference between the two.

4.2.2 Urban Test

Figure 29 shows a satellite image of the environment where the urban test was conducted, where blue dots marking where data points were collected, and red lines show straight lines to key points for discussion.

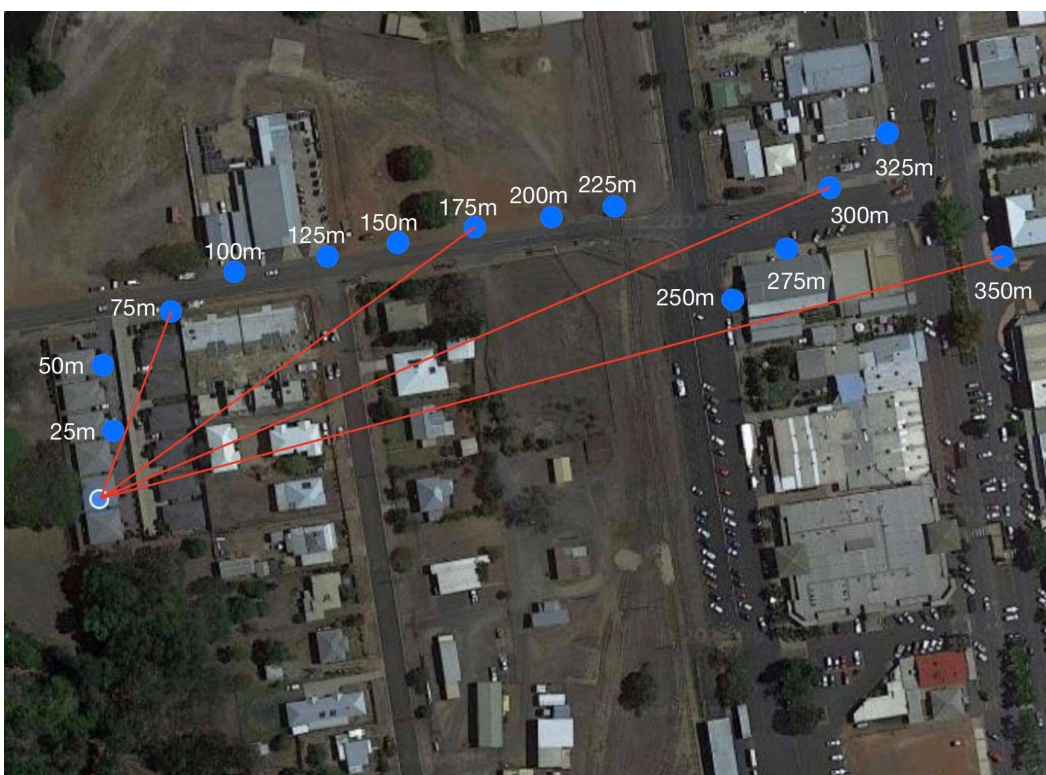


Figure 29 - Urban Test Data Point Map (Google Maps, 2022)

For each point, elevation remains constant, however, the amount of infrastructure obstructing the signal varies. Figure 24 shows RSSI plotted against distance for the urban test. Consistent with Figure 22, the urban test shows a graduate drop in RSSI over the first 150 meters before remaining largely constant. Figure 25 shows the SNR plotted against distance for the urban test. At the 175-meter point, the SNR shows a steep decrease. Looking at Figure 29, the direct line from node to gateway at this point passes through more infrastructure and trees than the points before, which explains the decrease. However, the 200-meter and 225-meter points both displayed higher SNR than 175-meter, while having more infrastructure to obstruct the

signal. This suggests that between the node and gateway at the 175-meter point displayed an anomalous piece of data. This could be due to other devices between the node and gateway adding to the noise in the result. It could also be due to the direction of the antennas on both the node and gateway. A slight difference in these could cause an unexpectedly worse reading. Throughout the entire test however, the trend shows that SNR decreases as the distance between the node and gateway, and the infrastructure obstructing the signal increase. This evidence suggests that infrastructure between the node and gateway has little to no effect on the RSSI but does cause a measurable decrease in SNR.

4.2.3 Bush Test

Figure 30 shows a satellite image of the environment where the bush test was conducted where blue dots marking where data points were collected, and red lines show straight lines to key points for discussion.



Figure 30 - Bush Test Data Point Map (Google Maps, 2022)

For each point, elevation remains constant, however, the amount of bush between the node and the gateway, obstructing the signal varies. Figure 26 shows the RSSI plotted against distance for the bush test. Similar to the free space and the urban tests, the RSSI in the bush test shows a gradual drop over the first 125 to 175 meters, before remaining mostly constant for the rest of the test. Figure 27 Shows the SNR plotted against distance for the urban test. Consistent with the urban test, this graph shows a steep decrease in SNR at the 175-meter point. As seen on Figure 30, the 150-meter point has significantly less bush obstructing the signal than the 175-meter point. Therefore, the evidence suggests that the increase in bush between the node and gateway are responsible for the decrease in SNR. Over the next 100 meters, SNR continues to drop, consistent with the increase in bush obstructing the signal. This evidence, consistent with the two previous tests, suggests that the environmental factors, in this case bush, obstructing the signal, have little to no effect on RSSI but cause significant, measurable decreases in SNR.

4.2.4 Summary

RSSI and SNR testing across these environments shows that environmental factors, including elevation and obstructing infrastructure/bush cause significant impacts on SNR but not RSSI, this correlates with existing research which shows that RSSI is affected mainly by distance (Yim et al., 2018). Figure 25 and Figure 27 show that SNR gets as low as -6.67dB and -6.33dB respectively before the node's signal can no longer be read by the gateway. This indicates that SNR is a more relevant indicator of the signal's maximum distance than RSSI. While RSSI remains constant at about 120dBm after the first 100 to 200 meters of each test, there does not seem to be any noticeable decrease prior to failure which can indicate a weak signal. Therefore, the evidence suggests it is a decrease in signal quality, not strength which leads to failure in LoRaWAN under these environments.

Table 1 - Summary of LoRaWAN Performance across Environments

Environment	Free Space	Urban	Bush
Maximum Signal Distance (m)	800	350	275
RSSI at 200m (dBm)	-112	-123	-124
SNR at 200m (dB)	8.75	-2.83	-2.08

Table 1 shows a brief summary of the results, showing maximum signal distance, and RSSI and SNR at 200 meters. The results show that LoRaWAN performance is significantly better without infrastructure or environment obstructing the signal. Under free space conditions, the node was able to transmit 800 meters (likely significantly more if tested further) compared to just 350 meters and 275 meters in urban and bush environments respectively. The results also suggest that signal quality is affected by environmental obstructions while signal strength is mainly dependant on distance. Urban and bush performance is largely similar with the exception of maximum distance where LoRaWAN was able to transmit a signal 75 meters further. This likely was due to the low volume of infrastructure blocking the signal as seen in Figure 29. LoRaWAN performance would likely be considerably worse in a more densely populated area.

Despite the significant bush coverage, the LoRaWAN node transmitting successfully up to 275 meters proves the concept of this design to be used as a wireless sensor network for early bushfire detection. To achieve further distances, a higher gain antenna can be used with the LoRa device which would increase SNR, in turn transmitting higher quality signals at further distances.

4.3 Thermal Switch Testing

Table 2 shows the results from the thermal switch test. It gives the time for the switch to close, current and voltage for both a 70-degree and 100-degree switch. As mentioned in methodology, power consumption is also calculated using Equation 1. The results show negligible differences between the switches in regard to power consumption, while the 100-degree switch takes 1.1 seconds more to close when heated by a lighter than the 70-degree switch.

Table 2 - Results of Thermal Switch Testing

Thermal Trip Temperature (°C)	70		100	
Switch Position	Open	Closed	Open	Closed
Current (mA)	0	54.2	0	53.9
Voltage (V)	0	8.19	0	8.19
Power Consumption (mW)	0	443.9	0	441.4
Time for switch to close (s)	4.8		5.9	

4.4 Thermal Switch Discussion

The results in Table 2 show that while the thermal mechanical switch is open, no power is consumed by the node. It also shows that when a flame was held beneath the switch, it closed the circuit, allowing the node to transmit a signal to the gateway. (FIGURE to be added), demonstrates the device successfully transmitting as a result of a flame closing the switch. This proves the viability of this switch to provide the device with zero-power usage prior to a fire event.

As mentioned in the literature review, a LoRaWAN smart sensor node, designed to operate in a deep sleep, powering up to transmit a signal each 10 minutes was able to achieve a 4.5-year battery life with a 2000mAh battery (Mayer et al., 2019). Table 2 shows that with the 100-degree switch, current is 53.9mA. Therefore, this device with a 2000mAh battery would last less than 38 hours before consuming the entire 9-volt battery. However, with the switch in the circuit, the node is able to consume no battery, meaning it essentially can operate indefinitely prior to damage caused by a fire.

Table 2 shows that where the switch has a thermal trip temperature of 70 degrees Celsius, a small flame from a lighter takes 4.8 seconds to close the switch. Where the thermal trip temperature is 100 degrees Celsius, it takes 5.9 seconds to close the switch. When selecting the thermal trip temperature for the switch, 2 factors are considered. Firstly, the temperature must be high enough that it will not be closed due to a hot ground temperature in the absence of a fire. Secondly, the temperature must be low enough that the switch will close, allowing for successful transmission to the gateway prior to any fire damage. As the higher trip temperature still closed within 5.9 seconds due to the small flame, it should be used with the final design. In the presence of a bushfire, the switch will close significantly faster, meaning there should be no damage to the node prior to the signal being sent. The higher trip temperature also prevents the device from incorrectly detecting a fire. As ground temperatures can get significantly higher than air temperature, the 70-degree switch suffers from this issue.

The node was constructed with a 100-degree switch and heated with the flame to test if a signal would successfully be received by the gateway. The results showed that it was able to accurately detect the fire and successfully transmit to the gateway, while consuming zero-power prior to fire detection.

Therefore, the results have clearly validated the near zero-power wireless sensor node for use in early bushfire detection.

5 CONCLUSIONS

The current solutions to early bushfire detection are either not effective enough or require frequent maintenance. Satellite detection suffers from cloud cover causing either phantom detection of fires or undetected fires while WSNs require frequent battery replacement. Therefore, a solution which can accurately detect bushfires and consumes near zero-power offers significant upside.

Hence, the aim of this thesis was to develop a wireless sensor node capable of detecting a fire and transmitting a long-range signal to a base station with zero power usage prior to fire detection and to evaluate its performance. This was achieved by conducting a literature review and establishing the best and most cost-effective solutions for both the long-range communication and zero power usage. LoRaWAN was selected for a low-power solution to long range communication and a thermal mechanical switch was selected so the device would consume no power prior to detecting a fire. The LoRaWAN node's performance was tested in a variety of environments and landscapes by measuring the RSSI and SNR over distance. The switch was evaluated by measuring power consumption prior to and after a fire as well as the time taken for the switch to close and validating that the node successfully transmitted when a fire was detected. Based on the results of this thesis, the following conclusions can be drawn:

1. Despite various environments obstructing the signal, the LoRaWAN node was able to reliably communicate with the gateway from long distances. Therefore, LoRaWAN offers a viable solution to low-power, long range communication. This allows the bushfire detection device to transmit long distance to a gateway, which then uploads the data, allowing the fire detection data to be analysed remotely.
2. Using the thermal mechanical switch, the node consumed no power prior to detection of a fire. A small fire was detected within 6 seconds, and the node successfully transmitted data to the gateway alerting of the fire. Therefore, the thermal mechanical switch is a viable solution for the bushfire detection device. It not only allows it to detect fire, but it offers zero power consumption prior to fire detection, essentially negating the need for any maintenance.

In summary, the device designed and tested in this report proves the concept of a WSN consisting of zero-power LoRaWAN nodes for use in early bushfire detection.

The main limitation of the device is its hindered performance through heavy bush. Though it was able to transmit a signal 275 meters, over a large bush covered area, this may not be adequate. Future work for this device can be done in two areas:

1. Developing a wireless sensor node capable of transmitting significantly further through heavy bush, while maintaining the low budget necessary for a WSN.
2. Researching a mesh solution based on the wireless sensor node designed in this thesis. Since the nodes use a zero-power switch, they cannot actively listen for a signal and therefore a mesh network cannot currently be achieved. A solution to this problem would allow for essentially unlimited range as the nodes could relay signals onward to the gateway.

6 REFERENCES

- A. M. A. Rahman, F. H. K. Zaman, S. A. C. Abdullah, "Performance analysis of LPWAN using LoRa technology for IoT application," *International Journal of Engineering and Technology (UAE)*, 2018, 7. 212-216, doi: 10.14419/ijet.v7i4.11.20808.
- B. Eric, "LoRa," *readthedocs.io*, 2018, doi: <https://lora.readthedocs.io/en/latest/#rss>
- D. Yim, J. Chung, Y, Cho, H. Song, D. Jin, S. Kim, S. Ko, A. Smith, A. Riegsecker, "An experimental LoRa performance evaluation in tree farm," *2018 IEEE Sensors Applications Symposium (SAS)*, 2018, pp. 1-6, doi: 10.1109/SAS.2018.8336764.
- Google Maps. "Butler Reserve". Satellite Image. 2022, <https://www.google.com/maps/@-16.9049433,145.7159868,450m/data=!3m1!1e3!5m1!1e4>. Accessed September 30, 2022.
- Google Maps. "Farmland, Bellenden Ker". Satellite Image. 2022, <https://www.google.com/maps/@-17.2989023,145.9243716,534m/data=!3m1!1e3!5m1!1e4>. Accessed September 30, 2022.
- Google Maps. "Mareeba". Satellite Image. 2022, <https://www.google.com/maps/@-16.9916761,145.420203,378m/data=!3m1!1e3!5m1!1e4>. Accessed September 30, 2022.
- G. M. Rebeiz, "RF MEMS switches: status of the technology," *TRANSDUCERS '03. 12th International Conference on Solid-State Sensors, Actuators and Microsystems. Digest of Technical Papers (Cat. No.03TH8664)*, 2003, pp. 1726-1729 vol.2, doi: 10.1109/SENSOR.2003.1217118.
- H. Jaafar, K. S. Beh, N. A. M. Yunus, W. Z. W. Hasan, S. Shafie, O. Sidek, "A comprehensive study on RF MEMS switch," *Microsyst Technol*, 2014, **20**, 2109–2121, doi: <https://doi.org/10.1007/s00542-014-2276-7>
- I. A. Csiszar, J. T. Morisette and L. Giglio, "Validation of active fire detection from moderate-resolution satellite sensors: the MODIS example in northern eurasia," *in*

IEEE Transactions on Geoscience and Remote Sensing, vol. 44, no. 7, pp. 1757-1764, July 2006, doi: 10.1109/TGRS.2006.875941.

J. Dozier, “A method for satellite identification of surface temperature fields of subpixel resolution,” *Remote Sensing of Environment*, 1981, 11, 221-229.

L. Casals, B. Mir, R. Vidal, C. Gomez, “Modeling the Energy Performance of LoRaWAN,” *Sensors*. 2017; 17(10):2364. <https://doi.org/10.3390/s17102364>

L. Giglio, W. Schroeder, C. Justice, “The collection 6 MODIS active fire detection algorithm and fire products,” *Remote Sens Environ* 178, 2016, pp. 31–41.
<https://doi.org/10.1016/j.rse.2016.02.054>

L. Hua, G. Shao, “The progress of operational forest fire monitoring with infrared remote sensing,” *J. For. Res.* 28, 2017, pp. 215–229, doi: <https://doi.org/10.1007/s11676-016-0361-8>

L. Yu, N. Wang, X. Meng, "Real-time forest fire detection with wireless sensor networks," *Proceedings. 2005 International Conference on Wireless Communications, Networking and Mobile Computing*, 2005, pp. 1214-1217, doi: 10.1109/WCNM.2005.1544272.

Z. Li, Y. J. Kaufman, C. Ichoku, R. Fraser, A. Trishchenko, L. Giglio, J. Jin, X. Yu, “A Review of AVHRR-based Active Fire Detection Algorithms: Principles, Limitations, and Recommendations,” *Canada Centre for Remote Sensing, Ottawa, Canada, K1A 0Y7*, 2001.

M. Antunes, L. M. Ferreira, C. Viegas, A. P. Coimbra and A. T. de Almeida, "Low- Cost System for Early Detection and Deployment of Countermeasures Against Wild Fires," *2019 IEEE 5th World Forum on Internet of Things (WF-IoT)*, 2019, pp. 418- 423, doi: 10.1109/WF-IoT.2019.8767331.

M. A. Finney, “The wildland fire system and challenges for engineering,” *Fire Safety J*, 2021, 120:103085

- M. I. Hossain, J. I. Markendahl, “Comparison of LPWAN Technologies: Cost Structure and Scalability,” *Wireless Pers Commun*, 2021, **121**, 887–903.
<https://doi.org/10.1007/s11277-021-08664-0>
- M. P. Martin, P. Ceccato, S. Flasse, I. Downey, “Fire detection and fire growth monitoring using satellite data,” In: Chuvieco, E. (eds) *Remote Sensing of Large Wildfires*. Springer, Berlin, Heidelberg, 1999, doi: https://doi.org/10.1007/978-3-642-60164-4_6
- N. Vatcharatiansakul, P. Tuwanut and C. Pornavalai, "Experimental performance evaluation of LoRaWAN: A case study in Bangkok," *2017 14th International Joint Conference on Computer Science and Software Engineering (JCSSE)*, 2017, pp. 1-4, doi: 10.1109/JCSSE.2017.8025948.
- P. Mayer, M. Magno, T. Brunner and L. Benini, "LoRa vs. LoRa: In-Field Evaluation and Comparison For Long-Lifetime Sensor Nodes," *2019 IEEE 8th International Workshop on Advances in Sensors and Interfaces (IWASI)*, 2019, pp. 307-311, doi: 10.1109/IWASI.2019.8791362.
- S. Devalal and A. Karthikeyan, "LoRa Technology - An Overview," *2018 Second International Conference on Electronics, Communication and Aerospace Technology (ICECA)*, 2018, pp. 284-290, doi: 10.1109/ICECA.2018.8474715.
- S. Jones, K. Reinke, S. Mitchell, F. McConachie, C. Holland, “Advances in the Remote Sensing of Active Fires: A Review,” *RMIT University*, 2017, doi: https://www.bnhcrc.com.au/sites/default/files/managed/downloads/2.2.3_advances_in_the_remote_sensing_of_active_fires_report_v1.0.pdf
- U. Dampage, L. Bandaranayake, R. Wanasinghe, K. Kottahachchi, B. Jayasanka, “Forest fire detection system using wireless sensor networks and machine learning,” *Scientific Reports*, 2022, doi: <https://doi.org/10.1038/s41598-021-03882-9>
- V. Rajaram, Z. Qian, S. Kang, N. E. McGruer, M. Rinaldi, “MEMS-based near-zero power infrared wireless sensor node,” *IEEE International Conference on Micro Electro Mechanical Systems*, 2018, pp 17-20

X. Li, L. Lang, J. Liu, Y. Xia, L. Yin, J. Hu, D. Fang, H. Zhang, “Electro-thermally actuated RF MEMS switch for wireless communication,” *2010 IEEE 5th International Conference on Nano/Micro Engineered and Molecular Systems*, 2010, 497-500.

Z. Chaczko, F. Ahmad, “Wireless Sensor Network Based System for Fire Endangered Areas,” *Proceedings - 3rd International Conference on Information Technology and Applications*, 2005, ICITA 2005. 203 - 207. 10.1109/ICITA.2005.313.

7 APPENDICES

7.1 Appendix 1 – Arduino IDE Code

7.1.1 LoRaWAN Shield Code

```
/*
```

LoRa Simple Client for Arduino :

Support Devices: LoRa Shield + Arduino

Example sketch showing how to create a simple messageing client, with the RH_RF95 class. RH_RF95 class does not provide for addressing or reliability, so you should only use RH_RF95 if you do not need the higher level messaging abilities.

It is designed to work with the other example LoRa Simple Server

User need to use the modified RadioHead library from:

<https://github.com/dragino/RadioHead>

modified 16 11 2016

by Edwin Chen <support@dragino.com>

Dragino Technology Co., Limited

```
*/
```

```
#include <SPI.h>
#include <RH_RF95.h>

// Singleton instance of the radio driver
RH_RF95 rf95;
float frequency = 915.0;

void setup()
{
    Serial.begin(9600);
```

```
//while (!Serial) ; // Wait for serial port to be available
Serial.println("Start LoRa Client");
if (!rf95.init())
    Serial.println("init failed");
// Setup ISM frequency
rf95.setFrequency(frequency);
// Setup Power,dBm
rf95.setTxPower(13);

// Setup Spreading Factor (6 ~ 12)
rf95.setSpreadingFactor(7);

//                                         Setup           BandWidth,          option:
7800,10400,15600,20800,31200,41700,62500,125000,250000,500000
//Lower BandWidth for longer distance.
rf95.setSignalBandwidth(125000);

// Setup Coding Rate:5(4/5),6(4/6),7(4/7),8(4/8)
rf95.setCodingRate4(5);
}

void loop()
{
    Serial.println("Sending to LoRa Server");
    // Send a message to LoRa Server
    uint8_t data[] = "Hello, this is device 1";
    rf95.send(data, sizeof(data));

    rf95.waitPacketSent();
    // Now wait for a reply
    uint8_t buf[RH_RF95_MAX_MESSAGE_LEN];
    uint8_t len = sizeof(buf);

    if (rf95.waitAvailableTimeout(3000))
```

```
{  
    // Should be a reply message for us now  
    if (rf95.recv(buf, &len))  
    {  
        Serial.print("got reply: ");  
        Serial.println((char*)buf);  
        Serial.print("RSSI: ");  
        Serial.println(rf95.lastRssi(), DEC);  
    }  
    else  
    {  
        Serial.println("recv failed");  
    }  
}  
else  
{  
    Serial.println("No reply, is LoRa server running?");  
}  
delay(5000);  
}
```

7.1.2 LoRaWAN Gateway Code

```
/*  
LoRa Simple Yun Server :  
Support Devices: LG01.
```

Example sketch showing how to create a simple messaging server, with the RH_RF95 class. RH_RF95 class does not provide for addressing or reliability, so you should only use RH_RF95 if you do not need the higher level messaging abilities.

It is designed to work with the other example LoRa Simple Client

User need to use the modified RadioHead library from:

<https://github.com/dragino/RadioHead>

modified 16 11 2016

by Edwin Chen <support@dragino.com>

Dragino Technology Co., Limited

*/

//If you use Dragino IoT Mesh Firmware, uncomment below lines.

//For product: LG01.

#define BAUDRATE 115200

//If you use Dragino Yun Mesh Firmware , uncomment below lines.

//#define BAUDRATE 250000

#include <Console.h>

#include <SPI.h>

#include <RH_RF95.h>

#include <LoRa.h>

// Singleton instance of the radio driver

RH_RF95 rf95;

int led = A2;

float frequency = 915.0;

void setup()

{

pinMode(led, OUTPUT);

Bridge.begin(BAUDRATE);

Console.begin();

while (!Console) ; // Wait for console port to be available

Console.println("Start Sketch");

```
if (!rf95.init())
    Console.println("init failed");
// Setup ISM frequency
rf95.setFrequency(frequency);
// Setup Power,dBm
rf95.setTxPower(13);

// Setup Spreading Factor (6 ~ 12)
rf95.setSpreadingFactor(7);

//                                         Setup           BandWidth,          option:
7800,10400,15600,20800,31200,41700,62500,125000,250000,500000
rf95.setSignalBandwidth(125000);

// Setup Coding Rate:5(4/5),6(4/6),7(4/7),8(4/8)
rf95.setCodingRate4(5);

Console.print("Listening on frequency: ");
Console.println(frequency);
}

void loop()
{
    if (rf95.available())
    {
        // Should be a message for us now
        uint8_t buf[RH_RF95_MAX_MESSAGE_LEN];
        uint8_t len = sizeof(buf);
        if (rf95.recv(buf, &len))
        {
            digitalWrite(led, HIGH);
            RH_RF95::printBuffer("request: ", buf, len);
            Console.print("got request: ");
            Console.println((char*)buf);
        }
    }
}
```

```
Console.print("RSSI: ");
Console.println(LoRa.packetRssi());
Console.print("SNR: ");
Console.println(LoRa.packetSnr());

// Send a reply
uint8_t data[] = "And hello back to you";
rf95.send(data, sizeof(data));
rf95.waitPacketSent();
Console.println("Sent a reply");
digitalWrite(led, LOW);
}

else
{
    Console.println("recv failed");
}
}

}
```

7.2 LoRaWAN Distance Testing Results

7.2.1 Free Space Test Results

Table 3 - LoRaWAN Free Space Test Raw Data

Distance (m)	Test 1		Test 2		Test 3	
	RSSI	SNR	RSSI	SNR	RSSI	SNR
0	-54.00	9.75	-54.00	9.75	-58.00	9.50
25	-87.00	9.75	-90.00	9.75	-95.00	9.50
50	-88.00	9.25	-92.00	10.00	-90.00	9.50
75	-98.00	9.75	-99.00	9.00	-97.00	9.75
100	-102.00	9.75	-102.00	9.50	-101.00	9.50
125	-103.00	9.75	-104.00	9.25	-104.00	9.50

150	-114.00	7.25	-117.00	5.75	-111.00	8.50
175	-110.00	9.00	-113.00	9.00	-108.00	9.00
200	-114.00	8.75	-111.00	8.75	-111.00	8.75
225	-110.00	8.50	-117.00	6.00	-118.00	5.50
250	-123.00	-1.00	-117.00	6.50	-118.00	5.50
275	-118.00	6.25	-117.00	6.50	-116.00	7.25
300	-112.00	8.50	-114.00	8.00	-112.00	8.50
325	-114.00	7.75	-115.00	7.75	-114.00	8.50
350	-112.00	7.75	-111.00	8.75	-110.00	8.75
375	-122.00	1.50	-126.00	-5.00	-125.00	-1.25
400	-115.00	5.50	-115.00	6.00	-114.00	6.00
425	-124.00	-4.00	-125.00	-5.00	-127.00	-3.50
450	-123.00	2.50	-123.00	3.25	-125.00	-1.50
475	-120.00	5.75	-120.00	5.25	-119.00	5.50
500	-121.00	2.75	-123.00	2.50	-123.00	1.50
525	-118.00	6.75	-119.00	5.25	-117.00	6.00
550	-123.00	2.00	-119.00	6.75	-125.00	-0.50
575	-123.00	1.75	-119.00	6.25	-121.00	4.00
600	-120.00	5.75	-121.00	4.00	-120.00	5.50
625	-126.00	-4.75	-120.00	5.00	-121.00	4.25
650	-113.00	9.00	-122.00	4.00	-121.00	4.50
675	-114.00	8.75	-116.00	7.50	-117.00	7.25
700	-126.00	-3.25	-113.00	8.75	-117.00	7.75
725	-120.00	7.25	-120.00	6.75	-119.00	7.50
750	-118.00	7.00	-120.00	6.75	-121.00	8.00
775	-119.00	7.25	-115.00	7.50	-115.00	7.50
800	-121.00	7.25	-119.00	7.25	-122.00	6.75

7.2.2 Urban Test Results

Table 4 - LoRaWAN Urban Test Raw Data

Distance (m)	Test 1		Test 2		Test 3	
	RSSI	SNR	RSSI	SNR	RSSI	SNR
0	-56.00	9.00	-55.00	9.50	-57.00	9.75
25	-94.00	9.50	-99.00	9.25	-97.00	9.50
50	-102.00	9.00	-111.00	8.75	-107.00	9.25

75	-95.00	10.00	-116.00	5.50	-115.00	6.75
100	-112.00	7.50	-119.00	1.50	-115.00	6.25
125	-117.00	5.25	-115.00	6.50	-117.00	5.25
150	-119.00	4.00	-122.00	1.75	-119.00	4.25
175	-124.00	-6.25	-124.00	-1.50	-123.00	-4.50
200	-124.00	-5.00	-123.00	-3.75	-122.00	0.25
225	-116.00	7.00	-123.00	-3.00	-124.00	-6.50
250	-124.00	-6.00	-122.00	0.00	-122.00	-2.50
275	-123.00	-5.25	-123.00	-2.75	-122.00	-1.00
300	-123.00	-5.75	-125.00	-3.50	-121.00	-1.50
325	-124.00	-4.75	-124.00	-7.50	-124.00	-5.75
350	-124.00	-5.00	-123.00	-8.00	-125.00	-7.00

7.2.3 Bush Test Results

Table 5 - LoRaWAN Bush Test Raw Data

Distance (m)	Test 1		Test 2		Test 3	
	RSSI	SNR	RSSI	SNR	RSSI	SNR
0	-50.00	9.00	-51.00	9.75	-56.00	9.50
25	-89.00	9.75	-88.00	9.50	-87.00	10.00
50	-87.00	9.75	-88.00	9.50	-94.00	9.50
75	-102.00	9.50	-97.00	9.50	-97.00	9.50
100	-103.00	9.50	-105.00	9.25	-107.00	9.75
125	-122.00	7.75	-117.00	7.25	-112.00	8.25
150	-114.00	7.00	-111.00	7.50	-111.00	8.75
175	-120.00	2.75	-125.00	-5.00	-124.00	-1.75
200	-124.00	-1.75	-124.00	-2.50	-124.00	-2.00
225	-125.00	-2.75	-126.00	-3.75	-125.00	-3.25
250	-127.00	-5.00	-126.00	-6.00	-127.00	-6.75
275	-127.00	-7.75	-127.00	-5.00	-127.00	-6.25